Number and proportion of *P. falciparum* gametocytes vary from acute infection to chronic parasite carriage despite unaltered sexual commitment rate

Hannah van Dijk[1], Nathalia F Lima[1], Martin Kampmann[2], Michael Gabel[3], Usama Dabbas[1,2], Safiatou Doumbo[4], Hamidou Cisse[4], Shanping Li[5], Myriam Jeninga[6], Richard Thomson-Luque[1], Didier Doumtabe[4], Michaela Petter[6], Kassoum Kayentao[4], Aissata Ongoiba[4], Teun Bousema[7], Peter D Crompton[5], Boubacar Traore[4], Frederik Graw[3,8], Silvia Portugal[1,2*]

[1] Center for Infectious Diseases, Parasitology, Heidelberg University Hospital, Heidelberg, Germany

[2] Max Planck Institute for Infection Biology, Berlin, Germany

[3] BioQuant-Center for Quantitative Biology, Heidelberg University, Heidelberg, Germany

[4] Mali International Center of Excellence in Research, University of Sciences, Techniques and Technologies of Bamako, Mali

[5] Laboratory of Immunogenetics, National Institute of Allergy and Infectious Diseases, National Institutes of Health, Rockville, Maryland, USA

[6] Mikrobiologisches Institut-Klinische Mikrobiologie, Universitätsklinikum Erlangen

[7] Radboud University Medical Center, Nijmegen, the Netherlands

[8] Interdisciplinary Center for Scientific Computing, Heidelberg University, Heidelberg, Germany

[*]Corresponding author email: portugal@mpiib-berlin.mpg.de (SP)

The authors declare no conflict of interest

Abstract

Introduction In areas of seasonal malaria, resuming transmission every wet season relies on persistent asexual parasites during dry season that maintain the ability to produce gametocytes until the mosquito population resurges following the start of annual rains. Although human asymptomatic *P. falciparum* reservoirs in the dry season are widely recognized, the longitudinal dynamics of parasite sexual commitment and gametocytogenesis remain unclear.

Methods We compared the expression of genes related with sexual commitment and gametocytogenesis of *P. falciparum*, the density and proportion of *P. falciparum* gametocytes, and the blood concentrations of phospholipids potentially involved in gametocytogenesis from asymptomatic subjects at the end of the dry season versus subjects with symptomatic malaria in the wet season. Furthermore, we verified whether number and proportion of gametocytes in asymptomatic vs clinical cases had similar trends in areas of seasonal and perennial transmission settings. Finally, we adapted a within-host mathematical model considering asexual parasites, sexually committed parasites, and gametocytes to infer the dynamics of gametocyte number and proportion as *P. falciparum* infections progress.

Results We found that transcripts of genes specific of late-stage gametocytes were predominantly upregulated in asymptomatic infections at the end of the dry season, which also showed increased proportions of circulating mature gametocytes compared to clinical malaria cases. On the other hand, blood densities of gametocytes and asexual parasites were lower in chronic asymptomatic individuals compared to clinical malaria. In addition, the levels of parasite transcripts involved in sexual commitment were unaltered throughout the year.

Discussion Our experimental data in combination with mathematical modelling support a scenario in which gametocyte density and proportion diverge as infections progress from recent transmission to chronic carriage, without significant alterations in the rate of sexual commitment over time.

Key words *Plasmodium*, *P. falciparum*, gametocytes, dry season, asymptomatic, parasite sexual commitment, malaria mathematical model

52

53 **Introduction**

54 It has long been known that the malaria-causing parasite *Plasmodium falciparum* requires a
55 mosquito host to complete its lifecycle and to be transmitted between humans (1). However, it
56 remains unclear if, in the human host, the parasite can dynamically allocate resources to the
57 differentiation of sexual-stage gametocytes that are transmitted to mosquitos, particularly in areas
58 of seasonal malaria where the size of the mosquito population fluctuates dramatically during the
59 dry and wet seasons. During blood feedings, infected Anopheles mosquitoes deposit *P. falciparum*
60 sporozoites in the human dermis that find their way into circulation, reaching the liver where they
61 infect hepatocytes. After 7-10 days of parasite replication, each infected hepatocyte releases
62 thousands of merozoites into the blood stream (2), where they start continuous asexual intra-
63 erythrocytic replication cycles of ~48 h, from merozoite invasion of red blood cells (RBCs), through
64 the ring- and trophozoite-stages, until the multinucleated schizont releases new merozoites (3). A
65 small proportion of intra-erythrocytic asexual parasites differentiate into sexual-stage gametocytes
66 (4). Instead of another ~48 h asexual schizogony leading to the 8-30 new merozoites ready to
67 continue asexual cycles (5), the parasite subsequently develops into sexually committed schizonts
68 leading to 8-30 sexually committed merozoites. Upon infection of new RBCs each sexually
69 committed merozoite produces one stage I gametocyte (6, 7) that through a period of 8-12 days
70 will go through five developmental stages (8), where nuclear reshaping is driven by intranuclear
71 microtubules (9, 10). Stages II to IV of gametocytaemia take place in the bone marrow or spleen
72 (11, 12), while stage V gametocytes are again present in peripheral blood, each lasting up to ~20
73 days (13, 14) waiting for another mosquito bite. Following a blood meal gametocytes encounter the
74 right environment for sexual reproduction in the mosquito midgut (15). They transform into female
75 and male gametes that fuse into a zygote originating oocysts which invade the midgut wall to
76 generate sporozoites. These sporozoites later reach the mosquito salivary glands and can restart
77 the parasite lifecycle after being taken up in the next blood meal (16). The continued presence of
78 mosquitoes and humans in a geographical region allows for perennial *P. falciparum* transmission.

79 However, in areas where the dry season is several months long, the mosquito population can
80 plummet to near zero (17), interrupting transmission. *P. falciparum* faces the challenge of surviving
81 in its human host for months while waiting for the return of mosquitoes as the wet season ensues
82 (18-20). During mosquito-free dry periods, gametocyte production is largely wasted, as
83 gametocytes cannot survive to bridge two wet seasons (13, 14). Although curtailing gametocyte
84 production rates during the dry season would seem beneficial to the parasite, such a strategy
85 would require a mechanism to reactivate gametocytogenesis with the return of rain and mosquitos.
86 Host factors such as age (21), haematocrit (22), haemoglobin type (23) and duration of malaria
87 symptoms (24) have been linked to gametocytaemia in individuals with clinical malaria; and higher
88 frequencies of gametocyte positive individuals have been observed in chronic asymptomatic
89 infections compared to acute infections (25-28). Additionally, various in vitro conditions have been
90 shown to modulate sexual commitment and thus gametocytogenesis (6, 29-31). The specific effect
91 of lysophosphatidylcholine (Lyso-PC) in repressing the pro-sexual commitment transcription factor
92 AP2G has been recently identified, with low Lyso-PC concentrations increasing the proportion of
93 sexual forms in vitro (31). Furthermore, gametocyte development 1 (GDV1) has been identified as
94 the de-repressing effector which counters the epigenetic silencing and promotes AP2G expression
95 leading to the induction of gametocytogenesis (32), and homeodomain protein 1 (HDP1) was
96 recently identified as a positive transcriptional regulator essential for gametocyte development (33).
97 Still, it is not fully understood how sexual investment and gametocytaemia is regulated in vivo, and
98 if or how transmission to mosquitoes can be optimized by the parasite to conserve resources.
99 Recently, we have shown that *P. falciparum* parasites isolated at the end of the dry season are
100 transcriptionally distinct from those of subjects with febrile malaria in the transmission season (18,
101 34), but alteration of sexual commitment and gametocytogenesis were not investigated. The
102 observed transcriptional differences reflected longer parasite circulation within each ~48 h intra-
103 erythrocytic cycle in the dry season, likely increasing splenic clearance of infected cells and thus
104 maintaining the low parasitaemias observed during the dry season (18). Here, we aimed to
105 examine sexual commitment and gametocytogenesis of parasites persisting through the dry

106 season and explored possible parasite adaptations during extended periods in the human host. We
107 quantified sexual commitment and female and male gametocyte densities in blood samples
108 collected from children at different times of the year with different clinical presentations and
109 seasonality patterns, and related them to total parasite density and infection length. Furthermore,
110 we determined longitudinally the Lyso-PC concentration in plasma of children, and assessed its
111 ability to induce *P. falciparum* sexual commitment and gametocytogenesis in vitro. Finally, we
112 adapted a previously described within-host mathematical model that considers asexual parasites,
113 sexually committed parasites, and gametocytes (35) to infer the dynamics of gametocyte number
114 and proportion as *P. falciparum* infections progress from recently transmitted to chronic
115 asymptomatic carriage over several months.
116
117 **Materials and Methods**
118 **Gametocyte gene expression analysis.** We used RNAseq data of leucocyte-depleted blood
119 pellets from 12 children with asymptomatic malaria at the end of the dry season and an age- and
120 gender-matched cohort presenting with their first malaria case in the ensuing transmission season
121 reported in (18). Originally 808 gametocyte specific genes were reported (36), and we counted 786
122 after excluding repetitions and converting nomenclature to its most recent version (Supplementary
123 Table 1). Out of these 786 genes, we detected normalized reads of 333 gametocyte-specific genes
124 in the RNAseq data set (18) to perform a principal component analysis. Using Deseq2, 205 genes
125 were determined to be differentially expressed between the dry season and malaria cases.
126
127 **Analysis of early and late gametocyte markers in RNA-seq data.** We compiled a list of early
128 and late gametocyte specific genes based on three RNA-seq studies comparing distinct parasite
129 stages, including data from Poran et al. 2017(37) obtained after request from the corresponding
130 author (compared day 2 versus day 9 of gametocytogenesis by single cell RNAseq); data from
131 Lopez-Barragan et al. 2011 (38) (compared day 4 versus day 15 of gametocytogenesis by bulk
132 RNAseq) and data from Jeninga et al., *under review* (compared day 4 of gametocytogenesis

133 versus day 10 of FACS sorted male and female gametocytes by bulk RNAseq). Poran et al.
134 selected early and late gametocyte genes as genes showing a 20-fold higher expression in early or
135 late gametocytes over the respective other group. Late gametocyte genes were also required to
136 show a 20-fold higher expression in late gametocytes compared to ring stage parasites, this was
137 not the case for early gametocyte genes. In Lopez-Barrgagan's data, early gametocyte genes were
138 defined as genes having a 10-fold expression increase in early gametocytes compared to late
139 gametocytes. Genes showing a 20-fold higher expression in late stages were designated as late
140 gametocyte genes. Expression differences to asexual stages were not considered. In Jeninga et al.
141 *under review* genes showing a 3-fold or higher expression difference to both asexual stages and
142 late gametocytes were selected as early gametocyte genes, regardless of gametocyte sex.
143 Intersecting the full list of early and late gametocyte genes with genes transcribed in circulating
144 parasites stages, defined by RNAseq data of Andrade et al., generated a final list of 109 early
145 gametocyte genes and 54 late gametocyte genes to evaluate expression differences of these
146 genes between dry and rainy seasons. Intersecting the early and late gametocyte list with all
147 gametocyte genes reported by Painter et al. we receive 456 gametocyte genes that are detected in
148 the wet vs dry season RNAseq dataset.
149
150 **Study subjects and ethical approval.** Approval by the Ethics Committee of Heidelberg University
151 Hospital, the Faculty of Medicine, Pharmacy and Odontostomatology (FMPOS) at the University of
152 Bamako, and the National Institute of Allergy and Infectious Diseases of the National Institutes of
153 Health Institutional Review Board was obtained to conduct the study registered at ClinicalTrials.gov
154 with the identifier NCT01322581. Clinical data and samples were obtained from 2017 to 2019 in a
155 cohort study previously described (39), conducted in Kalifabougou, Mali, where malaria
156 transmission occurs between June and December, and antimalarial drugs are provided by a single
157 clinic and pharmacy. All participants and the parents/guardians of included children provided
158 written informed consent. Exclusion criteria at enrolment included haemoglobin <7 g/dL, axillary
159 temperature ≥37.5°C, acute systemic illness, or use of antimalarial or immunosuppressive

160 medications in the 30 days preceding enrolment. Clinical malaria cases were prospectively
161 determined by passive surveillance and defined by axillary temperature ≥37.5°C, ≥2500 asexual
162 parasites/µL of blood, and no other evident cause of fever. Malaria episodes were treated with a 3-
163 day standard course of artemether/lumefantrine according to Malian national guidelines. Cross-
164 sectional clinical visits and blood draws were performed late in the transmission season (October),
165 and at the beginning (January), mid (March) and end (May) of the dry season.
166
167 **Sample collection.** Venous blood (4 mL if donor age was below 4 years, and 8 mL if above) was
168 drawn by venepuncture on wet and dry season cross-sectional visits, and at first malaria episode of
169 the transmission season. Samples are referred as MAL for malaria cases or by time point of
170 collection. Blood was collected in sodium citrate-containing cell preparation tubes (Vacutainer CPT
171 Tubes, BD) and transported to the laboratory where RBC pellet and plasma were separated and
172 stored at −80°C within three hours of blood draw. Plasma used for lipidomic analysis and induction
173 of gametocytogenesis was separated by centrifugation and immediately frozen in liquid N_2.
174
175 **RNA extraction and quantification of parasite transcripts.** RNA was isolated from 200 µl RBC
176 pellet by phenol-chloroform extraction using TRIzol (Ambion), followed by DNAse treatment using
177 the DNAse I Amplification Grade Enzyme (Invitrogen). RNA was quantified by absorption
178 measurements at 230, 260 and 280 nm on a Citation3 Imaging plate reader, followed by cDNA
179 synthesis using the Superscript IV Enzyme (Invitrogen) according to manufacturer instructions.
180 Taqman RT-qPCR multiplex assay (Applied Biosystems) was performed on a qTower (Analytic Jena)
181 with primers to quantify the female gametocyte marker ookinete surface protein P25
182 (PF3D7_1031000), the male gametocyte transcript PFMGET (Pf3D7_1469900), the master
183 regulator of sexual commitment Ap2G (PF3D7_1222600) and a parasite housekeeping gene
184 (Glycine-tRNA ligase, PF3D7_1420400). Amplification efficiency (E) was estimated on the basis of
185 the equation E=(10^(-1/slope)-1)x100 (Supplementary Figure 1). NF54 parasite line expressing
186 DyneinGFP and carrying an episomal P47mCherry plasmid (DynGFP/P47mCherry) was used for

187 sorting of male and female gametocytes through their respective specific mCherry and/or GFP
188 expression (40). Standard curves of 10-10^6/ml of sorter-purified female or male gametocytes were
189 generated by 10-fold serial dilution in 50% haematocrit (Supplementary Figure 1). qPCR expression
190 of female-specific P25 in female (mCherry+) sorted parasites was high and decreased with
191 gametocyte densities, while male gametocytes (GFP+) show ~12-fold lower expression of P25,
192 which may be explained by ~6% impurity originating from the opposite sex during sorting
193 (Supplementary Figure 1). Likewise, PfMGET expression was approximately 10-fold higher
194 expressed in male gametocytes (GFP+) compared to females (mCherry+), consistent with 5-7%
195 impurity. Linear regression fit for the independent populations revealed a good fit with R^2-values of
196 0.93-0.97 by P25 expression and 0.96-0.98 by PfMGET expression (Supplementary Figure 1). The
197 asexual parasites standard curve, was generated with Pf2004 asexual culture was counted by FACS
198 and Glycine-tRNA ligase expression was quantified in dilution series of 10-10^7 asexual late rings per
199 ml. The combination of asexual and sexual standard curves was used for qPCR quantification of
200 female or male proportion of total parasitaemias throughout the season. To account for fluorescence
201 leakage between channels a compensation matrix was calculated based on single colour
202 fluorescence measurements by an application specialist at Analytic Jena. Gexp5 (PF3D7_0936600)
203 expression levels were quantified in a Taqman RT-qPCR duplex assay together with Glycine-tRNA
204 ligase as a housekeeping gene. Expression levels of GDV1 (PF3D7_0935400), and MRSP1
205 (PF3D7_1335100) were determined in further Taqman RT-qPCR assays. All primers and probes
206 sequences are listed in Supplementary Table 2. Relative quantification was performed by ΔΔCt
207 method using Glycine-tRNA ligase as housekeeping gene and MAL samples a calibrator group.
208
209 **Parasite culture and preparation of a standard curve for gametocyte quantification.** Pf2004
210 parasites were cultured at 37° C in 5% O_2, 5% CO_2 and 90% N_2, at 5% haematocrit in RPMI-1640
211 medium (with L-glutamine and HEPES (Gibco)). Parasite culture medium was supplemented with
212 0.24% Sodium Bicarbonate (Gibco), 100µM Hypoxanthine (cc pro), 25 µg/mL gentamycin (Gibco)),
213 and 0.25% Albumax II (Gibco). Medium was changed daily, parasitaemia assessed by Giemsa-

214 stained blood smear and the culture split according to experimental needs.
215 *PfDyn*GFP/*PfP47*mCherry parasite lines (41) were cultured in presence of 15 µg/ml of Blasticidin-
216 S-HCL (Invitrogen) and 2 µM Pyrimethamine (Sigma Aldrich) as described for non-integrating
217 plasmids and P52 integrating plasmid. Parasites were grown to >4% parasitaemia when 50 mM N-
218 Acetylglucosamine (Sigma Aldrich) was added to the culture to eliminate asexual stages. After 4
219 consecutive days of N-Acetylglucosamine treatment, culture in complete RPMI was resumed.
220 Gametocyte development was monitored daily by smear, and on day 5 after start of gametocyte
221 induction magnetic enrichment was performed with MACS columns (Miltenyi Biotec). Gametocytes
222 were sorted on a BD FACSAria III on day 8, keeping cells at 4° C in suspended activation buffer,
223 (gating strategy in Supplementary Figure 1). RNA of a defined numbers of sorted male and female
224 gametocytes was extracted and reverse transcribed, a standard curve prepared by serial dilution
225 and used for RT-qPCR as described above.
226
227 **Phospholipid analysis.** May and MAL plasma samples (shown in Figure 1) were analysed by
228 shotgun lipidomics at Lipotype as described in (42). Briefly, automated samples extraction was
229 followed by direct sample infusion and high-resolution Orbitrap mass spectrometry including lipid
230 class-specific internal standards to assure absolute quantification of LysoPC and LysoPE, using
231 LipotypeXplorer for identification of lipids in the mass spectra. Oct, Mar, May and MAL samples
232 (shown in Supplementary Figure 4) were analysed by Liquid chromatography-mass spectrometry
233 (LC-MS). Samples were extracted, processed, and analysed at the Lipidomics Unit at the Institute
234 of Physiological Chemistry in Mainz, using the liquid-liquid extraction protocol as described (43). All
235 values were normalized to the analysed plasma volume.
236
237 **In vitro induction of *P. falciparum* sexual commitment and gametocytogenesis.** In vitro
238 induction of *P. falciparum* sexual commitment was performed as described by (Brancucci et al.,
239 2015). Pf2004 parasites were synchronized to a 4 h window by repeated treatment with 5% sorbitol
240 and MACS purification. Parasites at 26 ± 2 h post invasion (hpi) were plated on 48-well plates in

241 500 µl culture volume at 0.8-1% parasitaemia and 2.5% haematocrit and cultured in minimum fatty
242 acid medium (mFA, RPMI1640 with 100 µM hypoxanthine, 25 µg/ml gentamycin, 0.39% fatty-acid-
243 free BSA, 30 µM palmitic acid and 30 µM oleic acid) supplemented with 25% plasma from
244 asymptomatic children at the end of the dry season (PlMay), or 25% plasma from malaria cases
245 during the rainy season (PlMAL), in addition to the conditions used by Brancucci et al. (mFA alone,
246 and mFA supplemented with 25% German plasma (PlDE)). After 24 h of treatment, the medium
247 was changed to culture medium and subsequently changed daily. At 48 h after beginning of
248 treatment 30 IU/ml heparin were added to block re-invasion of parasites and eliminate asexual
249 forms. At 0, 48 and 120 h post treatment RBC pellets were collected for RNA quantification of
250 gametocyte markers by RT-qPCR; parasitaemia and gametocytaemia determination by flow
251 cytometry (50 µl of culture stained with 5x SYBR Green II (Invitrogen) and 7,5 µM MitoTracker
252 (Applied Biosystems) for 30 min at 37 °C and acquired with CountBright Absolute Counting Beads
253 (Thermo Ficher) on a FACS Canto II or an LSR II and analysed using FlowJo software 10.2 or
254 higher versions (Tree Star)). Additionally, Giemsa-stained blood smears were prepared at 48 h and
255 120 h post-treatment and blindly analysed by microscopy, counting RBCs, parasites, and
256 gametocytes in 18 fields of view. Multiplication rate of parasites was calculated as $\frac{parasitemia\ 48\ h}{parasitemia\ 0\ h}$,
257 and conversion rate as $\frac{gametocytemia\ 120\ h}{parasitemia\ 48\ h}$.
258
259 **Quantification of parasites in samples of Ugandan asymptomatic carriers by RT-qPCR.** We
260 compared the Malian data from dry and wet season with data from 150 Ugandan individuals
261 enrolled in a 2-year longitudinal study including monthly standardized clinical evaluation and blood
262 collection (44) retrieved from ClinEpiDB
263 (https://clinepidb.org/ce/app/record/dataset/DS_51b40fe2e2122). Asymptomatic *P. falciparum*
264 positive individuals (20.4 years ± 17.2, median: 13.3 years) were included based on the following
265 criteria: i) ≥ two PCR+ time points, ii) ≤ 3 negative time points in between positive, iii) same clone
266 (determined by deep amplicon sequencing of atypical membrane antigen 1 (AMA1) as described in
267 (45) present at all time points of one asymptomatic infection. Additionally, we used samples from

268 an age-matched group of 38 clinical malaria cases (tympanic temperature > 38°C or history of
269 fever in the previous 24 hours and *P. falciparum* positivity by microscopy). *P. falciparum* parasite
270 and gametocyte density in blood samples were measured by RT-qPCR of multi copy conserved
271 *var* gene acidic terminal sequence (46) and P25 (P25, PF3D7_1031000), respectively. Average
272 levels of parasitaemia and gametocytaemia during each asymptomatic infection, were estimated as
273 the area under curve over the course of infection divided by length of infection. For symptomatic
274 infections, only the quantification before treatment on day of diagnosis was considered. For
275 comparison between two data sets, a multiple non-parametric comparison between groups of
276 asymptomatic and symptomatic in Mali and Uganda has been performed using Tukey-Correction
277 for multiple comparisons.
278
279 **Mathematical model.** The developed mathematical model extends a model used previously to
280 describe asexual parasite and gametocytes dynamics (35). The model considers 3 different main
281 parasite populations, i.e., distinguishing between asexual parasites (P), sexually committed
282 parasites (P_G) and gametocytes (G). Asexual parasites develop and replicate within a red blood
283 cell over a cycle of length a_L=48h after which mature schizonts burst and release a number of r_P =
284 18-32 merozoites that are able to invade new red blood cells. During this replication cycle,
285 parasites are assumed to be removed through splenic clearance and active immune responses. In
286 extension to the previous model, we assume that this removal of asexual and committed parasites
287 follows an age dependent death rate, σ_a that differs in distinct phases of acute and chronic *P.*
288 *falciparum* infection. The following iterative equation describes asexual parasite growth at discrete
289 time steps for parasite age, *a*, and time, *t*, increments of one hour.

290
$$P(a,t) = \begin{cases} P(a-1,t-1)e^{-\sigma_a} \ , a = 2,3,\dots,a_L \\ r_p \ P(a_L,t-1)e^{-\sigma_a} \ , a = 1 \end{cases} \quad (1)$$

291
$$P(a_s + 1,t) = (1-f)P(a_s\,,t-1)e^{-\sigma_a} \quad (2)$$

The rate of parasite removal, σ_a, is assumed to increase with parasite age within one replicative cycle and is described by a sigmoidal curve given by:

$$\sigma_a = \sigma(a) = \frac{\sigma_{max}}{1+e^{p_\sigma(T_\sigma - a)}} \quad (3)$$

The parameter σ_{max} defines the maximal rate of parasite removal, T_σ the age at which 50% of parasites are removed, and p_σ a scaling parameter.

At parasite trophozoite stage of a_s= 20hpi parasites adhere to the endothelium when at the same time a fraction, f, of parasites enters sexual commitment. Committed parasites continue the rest of the replication cycle producing only committed parasites that enter the first gametocyte stage at the sequestration age, a_s, of the following replication cycle.

$$P_G(a_s+1,t) = f\,P(a_s,t-1)e^{-\sigma_a} \quad (4)$$

$$P_G\,(a,t) = \begin{cases} P(a-1,t-1)e^{-\sigma_a}, a = 2,3,\ldots,a_L \; except \; a = a_s \; and \; a = a_s+1 \\ r_p\;P(a_L,t-1)e^{-\sigma_a}\;, a = 1 \end{cases} \quad (5)$$

Gametocytes develop over 5 distinct stages of which only mature stage 5 is found in circulation. The development of gametocytes is then modelled by:

$$G_1(t) = G_1(t-1)e^{-(m-\delta_G)} + \frac{P_G(a_s-1,t-1)e^{-\sigma_a}(1-e^{-(m+\delta_G)})}{m+\delta_G} \quad (6)$$

$$G_2(t) = G_2(t-1)e^{-(m-\delta_G)} + \frac{mG_1\,(t-1)\,(1-e^{-(m+\delta_G)})}{m+\delta_G} \quad (7)$$

$$G_3(t) = G_3(t-1)e^{-(m-\delta_G)} + \frac{mG_2\,(t-1)\,(1-e^{-(m+\delta_G)})}{m+\delta_G} \quad (8)$$

$$G_4(t) = G_4(t-1)e^{-(m-\delta_G)} + \frac{mG_3\,(t-1)\,(1-e^{-(m+\delta_G)})}{m+\delta_G} \qquad (9)$$

308

$$G_5(t) = G_5(t-1)e^{-(\delta_{G5})} + \frac{mG_4\,(t-1)\,(1-e^{-(\delta_{G5})})}{\delta_{G5}} \qquad (10)$$

309

310 Immature gametocytes, that are sequestered, mature with a maturation rate, m, and are lost by
311 death rate δ_G , while mature circulating gametocytes are removed by a splenic clearance rate δ_{G5}.
312 As pointed out above the whole model is simulated by discrete time-steps of one-hour increments.
313 *Accounting for different phases of P. falciparum infection:* In our model the start of the infection is
314 marked by the beginning of blood stage infection, where we assume an initial parasite load, IPL,
315 with parasite age normally distributed with mean, μ_{IPL} and standard deviation σ_{IPL}. During the acute
316 phase of infection parasitaemias increase rapidly leading to clinical symptoms within the first 2
317 weeks of blood stage infection (47). The acute phase of infection is accompanied by the generation
318 of an adaptive immune response, including the production of effective antibodies, that takes ~14
319 days to develop (48). To account for higher parasite removal due to the immune response, we
320 assume an increased maximal parasite removal rate σ_{max2} for age-dependent parasite loss when
321 an adaptive immune response is active. Increased parasite removal is considered to occur 14 days
322 post start of blood stage malaria infection and indicates the beginning of the transition phase from
323 the acute towards the chronic asymptomatic phase of infection. In addition, as selection for less
324 adhesive and less virulent parasite strains by an active immune response is considered to be
325 crucial for the maintenance of a malaria infection over the course of several dry season months
326 (18), we accounted for this effect in our model by an increased value of T_σ for Eq. (3) during the
327 chronic asymptomatic phase, i.e., replacing T_σ by $T_{\sigma,2}$. Altering this parameter shifts clearance
328 rates towards affecting older asexual parasite stages, leading to a constant, but oscillating number
329 of asexual parasite numbers in circulation. *Parameter estimation*: The model described in Eqs (1-
330 10) was applied to the data assuming a fixed parasite life-cycle period of a_L=48 h, a sequestration

331 age of a_S= 20 hpi, as well as a parameter of T_σ=32 h and p_σ=0.7 characterizing age-dependent
332 parasite removal during the acute infection phase. All other parameters were fitted to both
333 symptomatic and asymptomatic time points simultaneously using an approximative Bayesian
334 computing approach (49). Prior distributions for the individual parameters spanning biologically
335 reasonable ranges have been selected in accordance with previous studies (Supplementary Table
336 3). Due to the high model complexity and parameter dependencies, estimations of multiple pyABC-
337 runs diverge to different local minima for the individual parameters. To obtain robust results for the
338 parameters indicating phase-dependent changes, several independent pyABC fitting runs were
339 compared and the 6th generation was chosen where parameter posterior distributions would still
340 overlap. For the fitting, values of individual patients in the dry season are condensed to one time
341 point by calculating the average levels based on the area under the curve over the course of dry
342 season patient surveillance. Values were log10-transformed to ensure comparability of
343 parasitaemia and gametocytemia. In addition, wet and dry season measurements were assumed
344 to represent the parasite dynamics at 2- and 6-weeks post infection, respectively. Sensitivity of the
345 results with regard to these time points was investigated. In addition, different values for the
346 fraction of sexually committed parasites, f, were tested. All code to run and analyse the
347 mathematical model is available at https://github.com/GrawLab/MalariaReplication.
348
349 **Supplementary Table 3.** List of model parameters and respective prior distributions. All prior
350 distributions were uniformly distributed given the indicated ranges.

Parameter	Unit	Description	Prior range	Ref for prior range	89% CI of post range
ipl	Parasite /ml	Initial parasite load	1 - 10	(Hodgson et al. 2015) (Schats et al. 2015)	1.47 - 6.54
μ_{ipl}	h	Initial parasite age	4 - 10	(Eichner et al. 2001)	4.41 - 8.22
σ_{ipl}	h	Standard deviation of initial parasite age	4.5 - 6.5	(Cao et al. 2019)	4.89 - 5.81
$\mathbf{r_p}$		Replication factor	18 - 32		2.28 - 3.13 x 10^1
σ_{max}	h^{-1}	Maximal removal rates during acute phase of infection	0.01- 0.15	(Andrade et al. 2020)	0.81 - 1.07 x10^{-1}
σ_{max2}	h^{-1}	Maximal removal rates during transition phase of infection	0.01- 0.4		2.13 - 2.39 x10^{-1}
δ_G	h^{-1}	Death rate immature gametocytes	1e-05 - 1e-04	(Cao et al. 2019)	3.53 - 8.60 x10^{-5}
δ_{G5}	h^{-1}	Death rate mature gametocytes	1.39 - 4.17 x10^{-3}	(Cao et al. 2019)	1.79 - 3.98 x10^{-3}
m	h^{-1}	Gametocyte maturation rate	1.6 - 4.6 x 10^{-2}	(Cao et al. 2019)	2.76 - 4.29 x10^{-2}

f	h^{-1}	Fraction of sexually committed parasites	0.5 - 1.0 x 10^{-2}	(Cao et al. 2019), (Eichner et al. 2001)	5.41 - 7.68 x10^{-3}
$\mathbf{a_L}$	h	Life cycle length	48		
$\mathbf{a_s}$	h	Sequestration age	20		
$\mathbf{T_\sigma}$	h	Age at which 50% of parasites are removed during acute phase of infection	32	(Andrade et al. 2020)	
$\mathbf{T_{\sigma 2}}$	h	Age at which 50% of parasites are removed during chronic phase of infection			33.6 - 34.7
$\mathbf{P_\sigma}$		Shape parameter	0.7	(Andrade et al. 2020)	
$\sigma_{max}/\sigma_{max2}$	h	Ratio of maximal removal rate	0.025 - 15		2.06 - 2.89

Results

***P. falciparum* transcription and quantification of gametocyte density and proportions.** We previously described differences in transcription between asexual *P. falciparum* of asymptomatic Malian children at the end of the dry season versus age- and sex- matched Malians presenting clinical malaria in the wet season (18), but we did not investigate transcripts specific to sexual forms of the parasite. Now, we gathered a list of genes related to gametocytogenesis from multiple RNAseq published and unpublished studies to query potential adaptations of *P. falciparum* sexual stages to persistence periods. Painter et al. reported, with in vitro culture parasites, 786 gametocyte-related transcripts (36), and of those 333 showed detectable number of reads in our dry vs wet season dataset (18) (Table 1 and Supplementary Table 1). Poran et al. described with single cell RNAseq analysis early and late gametocyte transcripts based on a 20-fold differential expression comparing day 2 versus day 9 of gametocytogenesis (late gametocyte genes were defined by 20-fold higher expression compared to ring stage parasites, although this was not the case for early gametocyte genes) (37). We found that 2 out of 3 transcripts and 15 out of 17 from early- and late-gametocyte transcripts, respectively, were detected at the end of our dry season asymptomatic versus wet season clinical case dataset (18) (Table 1 and Supplementary Table 1). In addition, data from Lopez-Barragan et al. 2011 compared bulk RNAseq of day 4 versus day 15 of gametocytogenesis and identified early-gametocyte genes through a 10-fold increase of expression in early compared to late gametocytes. Genes showing a 20-fold higher expression in late stages were designated as late-gametocyte genes, but expression differences to asexual stages were not considered (38). Forty-one and 58 transcripts were called early- and late-

373 gametocyte related genes (38) and of those 32 and 44 were detected in the end of our dry season
374 asymptomatic versus wet season clinical case dataset (18) (Table 1 and Supplementary table 1).
375 Finally, Jeninga et al. (personal communication, *under review*) obtained data comparing bulk
376 RNAseq data of day 4 versus day 10 of gametocytogenesis in FACS-sorted male and female
377 gametocytes defined early-female and early-male specific gametocyte transcripts with a 3-fold or
378 higher expression difference to both asexual stages and late gametocytes. Nineteen transcripts
379 were assigned to early gametocytes independent of sex, and 38 and 186 transcripts were identified
380 as early-female, and early-male gametocyte-related genes respectively. Of those, 15 and 64 were
381 detected at the end of our dry season asymptomatic versus wet season clinical cases dataset (18)
382 (Table 1 and Supplementary Table 1). The full list of 1048 sexual commitment- and
383 gametocytogenesis-related genes showed limited overlap between the different reports
384 (Supplementary Table 1) potentially due to the different timepoints and comparison conditions
385 defined in the different studies. Intersecting this list with transcripts of circulating parasites of the 12
386 asymptomatic Malians at the end of the dry season and 12 clinical malaria cases in the wet season
387 (18) resulted in 456 transcripts. Principal component analysis of expression values of these genes
388 showed a clear segregation of transcription profiles based on seasonality and clinical presentation
389 (Figure 1A), and produced clear patterns on a heatmap clustering malaria cases (MAL) or end of
390 the dry season asymptomatic samples (May) by similarity (Supplementary Figure 2). Of note,
391 transcripts characteristic of late stage gametocytes appeared especially enriched in upregulated
392 differentially expressed genes (DEGs) in samples of asymptomatic carriers in the dry season
393 versus malaria cases in the wet season. We identified 159 gametocyte-specific transcripts defining
394 early- or late-gametocyte development stages with quantifiable reads in samples of circulating
395 parasites persisting through the dry season and parasites causing malaria in the wet season (18).
396 Of those, 105 transcripts define early-stage gametocytes; and 54 transcripts are characteristic of
397 late-stage gametocytes (highlighted in Supplementary Table 1). Expression of these transcripts in
398 asymptomatic carriers at the end of the dry season (May) and malaria cases (MAL) in the wet
399 season showed an enrichment of upregulated transcripts of late-stage gametocytes in the dry

400 season. While 81,48% (44/54 genes, Chi^2 *p*-value < 0.00001) of late-stage gametocyte transcripts
401 were upregulated in the dry season, only 39,05% (41/105 genes, Chi^2 *p*-value = 0.231933) of
402 early-gametocyte transcripts and 33,4% (1131/3381 genes) of total *P. falciparum* transcripts were
403 upregulated in the dry season, respectively (Figure 1B). Transcripts of female (P25,
404 PF3D7_1031000) or male (PFMGET, Pf3D7_1469900) late stage gametocytes were upregulated
405 alongside other late sexual stage transcripts (highlighted in Supplementary Table 1), and P25
406 difference was also confirmed by qRT-PCR through the proportional quantification of female
407 gametocytes out of total parasites, while PFMGET qRT-PCR showed a non-significant trend of the
408 proportion of males out of total parasites between clinical malaria sample and asymptomatic at the
409 end of the dry season (Fig. 1C). On the other hand, transcripts known to regulate sexual
410 commitment (AP2G, PF3D7_1222600; and GDV1, PF3D7_0935400), to be present in sexually
411 committed schizonts (MSRP1, PF3D7_1335000), or to be markers of early gametocytes (GEXP5,
412 PF3D7_0936600) were not significantly different in the RNAseq analysis (highlighted in
413 Supplementary Table 1) nor qRT-PCR (Figure 1C). Decreased transcription of late-stage
414 gametocyte genes in symptomatic cases of malaria during the wet season coincided with lower
415 levels of phospholipids measured through shotgun lipidomics in the plasma of the same children
416 that is known to influence *P. falciparum* sexual commitment in vitro (31). Malaria cases in the wet
417 season (MAL) had lower levels of several species of the Lyso-PC (Figure 1D) and
418 lysophosphatidyle-thanolamine (Lyso-PE) (Figure 1D) families compared to asymptomatic carriers
419 at the end of the dry season (May). Decreasing Lyso-PC levels have been shown in vitro to
420 increase *P. falciparum* sexual commitment (31). Hence, we questioned if the reduction in Lyso-PC
421 and Lyso-PE species in plasma of malaria cases compared to persistent infections at the end of
422 the dry season could induce *P. falciparum* sexual conversion or gametocytaemia differently in vitro.
423 We exposed parasites of the *P. falciparum* 2004 line (Pf2004) to plasma of children collected
424 during clinical malaria cases (MAL) in the wet season, or to those of asymptomatically infected
425 children at the end of the dry season (May) alongside the conditions described by Brancucci et al.
426 (31) to induce or inhibit sexual convertion and gametocyteamia. As reported earlier (31), we

427 observed that 24 h after culturing Pf2004 without plasma or serum (noPl), and thus no Lyso-PC,
428 over minimal fatty acid medium (MFA), AP2G expression increased compared to parasites cultured
429 in the presence of German control plasma (PlDE) (Supplementary Figure 3). However, MFA
430 medium supplementation with 25% plasma from children presenting with clinical malaria in the wet
431 season (PlMAL), versus plasma from children with asymptomatic infections at the end of the dry
432 season (PlMay) resulted in similar APG2 induction 48 h after beginning of treatment
433 (Supplementary Figure 3), and similar conversion rate of parasites into gametocytes on day 5 after
434 treatment (defined by = d5gametocytes/ d2parasites) (Supplementary Figure 3). Absence of
435 plasma (noPl) resulted in higher gametocytaemia than observed within German pooled plasma
436 condition (PlDE) (Supplementary Figure 3), plasma from malaria cases (PlMAL) or asymptomatic
437 infections at the end of the dry season (PlMay), all revealing similar conversion rates. Although the
438 2-4 fold Lyso-PC differences between non-infected or asymptomatic children and malaria cases
439 were significant (Figure 1D), these were much lower than the several orders of magnitude included
440 in the standard curve used to establish that gametocyte conversion responds to decreasing Lyso-
441 PC in the culture medium (31).
442
443 ***P. falciparum* gametocyte density is higher in clinical cases of malaria than in asymptomatic**
444 **infection regardless of seasonality**
445 We determined the density of total *P. falciparum* parasites (Glycine-tRNA ligase,
446 PF3D7_1420400), female (P25, PF3D7_1031000) and male (PFMGET, Pf3D7_1469900)
447 gametocytes, based on standard curves obtained from total and sorted gender-specific fluorescent
448 gametocytes (40), respectively (Supplementary Figure 1), and detected higher numbers of both
449 total parasites, and of female and male gametocytes (Figure 2A) per mL of blood in clinical cases
450 of malaria during the wet season (MAL) compared to asymptomatic carriers at the end of the dry
451 season (May). This highlighted that the increased proportion of gametocytes shown by the over-
452 expression of transcripts of late stage gametocytes (Figure 1) was linked to lower parasite and
453 gametocyte densities in asymptomatic infections at the end of the dry season.

454 Furthermore, we determined the dynamics of *P. falciparum* sexual commitment and
455 gametocytogenesis in persistently infected individuals continuously infected throughout the dry
456 season. We quantified the density of total parasites, and fully formed female and male
457 gametocytes by qRT-PCR at four different time points in asymptomatic children persistently
458 infected from the wet (Oct) until the end of the dry season (through Jan, Mar and May), and in a
459 parallel group of age-matched individuals presenting with clinical malaria during the ensuing wet
460 season (MAL). We observed that total parasite density was higher in malaria cases (MAL) than at
461 any time-point of the asymptomatic infections, whether in the wet (Oct) or the dry season (Jan, Mar
462 and May). In contrast, no differences were found between any of the time points of asymptomatic
463 infections (Oct, Jan, Mar and May) (Supplementary Figure 4). Similarly, we observed higher
464 densities of both female and male gametocytes in malaria cases (MAL) than at any time point of
465 the asymptomatic infections (Oct, Jan, Mar and May), and no differences within the persisting
466 period (Supplementary Figure 4). Conversely, the proportion of male gametocytes was higher at
467 later time points of persisting infections (Mar or May) than in malaria cases during the transmission
468 season (MAL) (Supplementary Figure 4), while AP2G was again not found to significantly vary
469 across season or clinical presentation (Supplementary Figure 4). We also examined associations
470 between plasma Lyso-PC and Lyso-PE, monitoring longitudinally ~20 children who were
471 continuously infected from the wet season until the end of the dry season. Quantification of Lyso-
472 PC 18:0 in malaria cases compared to asymptomatic infections progressing from the wet into the
473 dry season again resulted in decreased Lyso-PC values in clinical malaria cases (MAL) compared
474 to asymptomatic infections (Oct, Mar and May) (Supplementary Figure 4). We further detected a
475 decrease of Lyso-PC from the wet season (Oct) to the end of the dry season (May), but no
476 difference was observed between the two available time points of the dry season (Mar and May)
477 (Supplementary Figure 4). Furthermore, Lyso-PC 18:0 levels in persistent infections (Oct, Mar and
478 May) were comparable to non-infected individuals at the end of the dry season (May^{-}), indicating
479 that asymptomatic infections have no impact on Lyso-PC 18:0 (Supplementary Figure 4).
480 Accordingly, a relation between Lyso-PC levels and parasitaemia or gametocytaemia was only

481 significant when considering clinical malaria plus all asymptomatic samples (Oct, Mar, May and
482 MAL) ($r=-0.68$ $p< 0.0001$; $r=-0.56$ $p< 0.008$ and $r=-0.67$ $p< 0.0001$ for parasitaemia, female and
483 male gametocytaemia respectively), but disappeared when each group was analysed
484 independently, or in all persisting asymptomatic infections analysed together (Supplementary
485 Figure 4).
486 Additionally, we investigated if the observed patterns of gametocyte densities and proportions were
487 generalizable to non-seasonal settings where infections also persist. While Mali shows a very
488 contrasting seasonal pattern with 5-6 months interruption of transmission every year (17), Uganda
489 has uninterrupted year-round transmission with peaks in times of stronger rain (44). RT-qPCR data
490 quantifying transcripts of total parasite (varATS) and gametocyte (P25, PF3D7_1031000) densities
491 from samples of 150 Ugandan individuals with asymptomatic parasitaemias persisting for over one
492 month (n=122) and age-matched individuals presenting with clinical malaria (n=38) had been
493 previously published (44) and were retrieved from ClinEpiDB (50). Determining average parasite
494 levels during the asymptomatic phase calculated by the area under the curve over the course of
495 infection normalized by the time of infection, indicated that parasite and gametocyte densities were
496 increased in clinical malaria cases (MAL) compared to asymptomatic infections (Asymp) (Figure
497 2B). In contrast, the proportion of gametocyte transcripts relative to total *P. falciparum* transcripts
498 showed again an inverse trend (Figure 2C), as seen within the Malian samples, where the
499 proportion of gametocytes was higher in persisting parasitaemias (Asymp) compared to malaria
500 cases (MAL) (Figure 1).
501
502 **Progressing infection leads to apparent differences in gametocytogenesis.** We observed
503 decreased densities but higher proportions of female or male gametocytes in asymptomatic versus
504 clinical malaria, without concomitant differences in the expression of regulators of sexual
505 commitment, or transcriptional markers of sexually committed schizonts or early gametocytes
506 (Figure 1, 2, Supplementary Figure 4 and Supplementary Table 1). Attempting to explain this, we
507 devised a mathematical model considering three different parasite populations - asexual parasites
508 (P), sexually committed parasites (P_G) and gametocytes (G), all of which can circulate or be

509 adherent - as previously developed (35) (Figure 3A). As the original model by Cao et al. (35) was
510 not able to sufficiently explain the observed dynamics when fitted to the data, we extended the
511 model in different ways. First, we incorporated our recent observation of increased clearance of
512 longer-circulating infected erythrocytes in persisting parasitaemias compared to recently
513 transmitted parasites (18), which promoted different removal rates of asexual and sexually-
514 committed parasites during distinct phases of acute and chronic *P. falciparum* infection (see
515 Methods and Source code 1). In addition, we distinguish between three phases *during P.*
516 *falciparum* infection in which the parasite multiplication factor varies due to immune response or
517 adhesive properties of the parasite, in agreement with a recent report (44) and Malian data
518 (Supplementary Figure 4). Using an iterative Bayesian fitting-approach to fit the model to the
519 symptomatic and asymptomatic parasitaemia and gametocytaemia levels of the Malian cohort, we
520 quantitatively assessed several biological parameters including sexual commitment rate,
521 gametocyte circulation time, parasite multiplication rate and gametocyte sequestration time,
522 thereby confirming previously determined ranges (35, 51) (Supplementary Figure 5). Our adapted
523 model was able to provide a dynamic depiction of parasitaemia levels, and gametocyte densities
524 and proportions, as we observed within the Malian data (Figure 3B). We found that the death rate
525 of asexual and sexually committed parasites increased at later stages of the 48 h cycle, shifting
526 toward the removal of older parasite stages and leading to a constant but oscillating number of
527 asexual parasite in circulation (highlighted in the box-inlay of Figure 3B). This oscillation, may be
528 explained by the variation seen in parasitaemias, especially during the chronic phase where we
529 pooled individual measurements collected across different time-points and calculated averages
530 from each individual by the area under the curve (see Methods). Keeping a constant fraction of
531 sexually committed parasites, f, throughout acute and chronic infection phases, our model predicts
532 a higher number and lower proportions of gametocytes in the acute phase - a trend that is inverted
533 during the transition phase of infection due to effective removal of asexual parasites by an active
534 immune response (Figure 3C and D). During the chronic phase of infection, when parasitaemias

535 remain constant or are slowly decreasing, gametocyte proportions are also decreasing until an
536 equilibrium is reached roughly 4-5 months after the start of blood stage infection.
537 Additionally, we tested the effect of increased sexual commitment during the chronic phase of
538 infection in our model. We observed that increasing sexual commitment We observed that
539 increasing sexual commitment from 0.54-0.76% (89% credibility interval of pyABC fitting approach)
540 to 2 or 20% during the chronic stage of infection led to steady and constant losses in parasitaemia,
541 which would, especially at very high sexual commitment rates, lead to parasite clearance and
542 substantially increased gametocyte proportions (Supplementary Figure 6). A high fraction of
543 sexually committed parasites during the chronic phase of infection would prevent a stable level of
544 parasitaemia over several months without reinfection. Overall, our model provides a dynamic
545 depiction of gametocyte densities and proportions as observed in the data from Mali and Uganda,
546 without the necessity to alter the sexual commitment rate (Fig 3C and D).
547
548 **Discussion**

549 The relative absence of mosquitoes during the months-long dry season and the short lifespan of *P.*
550 *falciparum* sexual-stage gametocytes (13, 14) renders the production of gametocytes ineffective
551 during most of the dry season. However, to ensure parasite reproduction, gametocytes must be
552 available to resume malaria transmission when mosquitos return with the wet season. Whether *P.*
553 *falciparum* maintains a constant rate of production of sexual forms or adjusts gametocytogenesis to
554 maximize transmission has been unclear. In this study, with samples from Malians exposed to
555 alternating 6-month dry and wet seasons, and samples from clinical malaria and asymptomatic *P.*
556 *falciparum* infection from year-round transmission region of Uganda, we showed that symptomatic
557 cases of malaria consistently have higher parasite and stage V gametocyte densities than
558 asymptomatic infections. However, the proportion of gametocytes is increased in the asymptomatic
559 persisting infections. Additionally, our data from Mali indicated that transcription of genes
560 characterizing sexually committed parasites and stage I gametocytes (52, 53) quantified by RT-
561 qPCR did not appear affected by the season or clinical symptoms (Figures 1 and 2), nor were
562 reads of over 100 genes characteristic of early gametocytes and detected by RNAseq of circulating

563 parasites particularly enriched for DEGs. This, clearly contrast with representative expressed
564 genes of late gametocytes that were very much enriched of transcripts upregulated in persisting
565 asymptomatic infections at the end of the dry season (Fig 1C and Supplementary Table 1).
566 Our work suggests that gametocytogenesis remains constant as infections progress from recent
567 transmission to chronic carriage, and it is the difference in asexual survival/replication rates that
568 promotes different gametocyte densities, independently of environmental factors.
569 Although it has been suggested that *P. falciparum* investment in gametocyte production adjusts to
570 host nutrient availability (54), drug pressure (24), transmission intensity (55), and even seasonality
571 (56, 57), results are often inconsistent and potentially affected by the dynamics of asexual parasite
572 growth, without necessarily indicating altered sexual commitment. In Sudan, following the long dry
573 season, gametocyte density estimates have been reported to increase prior to the highest
574 transmission peak (58), suggesting a higher gametocyte investment. However, in Burkina Faso,
575 gametocyte densities were higher at the peak and end of the transmission season rather than
576 during the dry season (59), while the efficiency of membrane feeding to infect mosquitoes was
577 increased early in the transmission season compared to peak of the malaria season or the dry
578 season (60). Nevertheless, these studies did not monitor longitudinally the same parasite
579 population during the dry and early wet season. In a recent study also in Burkina Faso,
580 transmission was shown to be more effective in persistent than in incident infections, but no data
581 was collected after day 35, and collections were all done during the wet season (25) when a mix of
582 more and less recently transmitted parasite clones is likely in individuals without symptoms.
583 In vitro, depletion of Lyso-PC or choline have been shown to induce AP2G expression, leading to
584 increased gametocyte production (31, 61), but associations in humans are inconsistent. In
585 Rwanda, low Lyso-PC associated with higher parasite densities (62); and in Ghana, although
586 correlations with parasitaemia were not reported, Lyso-PC levels in human blood samples were
587 inconsistently related with gametocyte-committed ring stages converting into gametocytes in vitro
588 (53). Our data show, like Orikiiriza et al.(62), an association of lower Lyso-PC levels with increased
589 parasitaemia and severity of malaria (Figure 1), but the association was lost at low parasitaemias,

590 and persistent infection at the end of the dry season did not affect Lyso-PC compared to non-
591 infected individuals (Supplementary Figure 4).
592 The effect of drugs on sexual conversion in vitro has been previously reported. Specifically, sub-
593 curative doses of dihydroartemisinin (DHA) stimulate AP2G expression and sexual conversion
594 when drug exposure occurs at the trophozoite stage, but not at the early ring stage. The observed
595 increase could not synergize nor add to increases promoted by depletion of choline, suggesting, as
596 DHA affects lipids, that the two effects might be the same (61). In vivo, it was recently shown that
597 soon after ART treatment AP2G transcripts increased in many but not all patients, and data
598 contrasted significantly between cohorts of different geographical regions, highlighting the complex
599 regulation of sexual conversion which is likely influenced by patient, parasite characteristics and
600 resistance status (63). Our RNAseq (S1 Table) and RT-qPCR (Fig 1H and 2D) data show constant
601 low-level expression of AP2G, the master regulator of gametocytogenesis, and equally unaltered
602 expression of transcripts characteristic of committed schizont and early gametocytes (S1 Table and
603 Fig 1H), suggesting that reductions in circulating Lyso-PC induced by uncomplicated clinical
604 malaria are not capable of affecting *P. falciparum* sexual commitment. Accordingly, we observed in
605 vitro that supplementation with plasma from clinical malaria cases (low Lyso-PC) or end of the dry
606 season persistently infected individuals (normal Lyso-PC) did not differentially induce AP2G
607 expression or the rate of sexual conversion (Fig 3), suggesting that Lyso-PC differences introduced
608 by *P. falciparum* infection are not sufficient to trigger the mechanisms demonstrated by Brancucci
609 et al. (31) and Portugaliza et al. (61). Nevertheless, it is possible that Lyso-PC levels in particular
610 bone marrow niches are sufficiently low to trigger parasites' sexual commitment, although this
611 would require that infected erythrocytes be at that niche to respond to the stimulus.
612 Previous reports highlighting differences in gametocytogenesis as a product of altered sexual
613 commitment did not account for longevity of infection, nor for dynamic changes within the asexual
614 compartment during a persistent infection. Greischar et al. demonstrated the difficulty of quantifying
615 true transmission investment by comparing existing quantification methods on simulated data
616 where true transmission investment is known (64), and Prajapati and colleagues relied on in vitro

617 culture of sexually committed circulating parasites to define samples with higher and lower
618 commitment rates (65). Also, our study has limitations as it is possible that our quantifications of
619 parasite and gametocyte densities are affected by imperfectly comparable primer efficiencies,
620 which would also affect comparisons of female, male and total gametocyte densities across
621 different transcripts measurements. Although we also do not have true longitudinal data, our model
622 can explain the observed patterns by assuming transitions from a faster to a slower growth rate, as
623 e.g. due to the development of immunity which has been recorded from malaria-therapy used to
624 treat neurosyphilis patients (66). Despite these limitations, our analyses show that the proportion of
625 sexual stages is inversely related in recent transmissions versus chronic infections, without
626 alteration in the expression of regulators of sexual commitment and while maintaining a constant
627 rate of sexual commitment. Our recent study in which we found that infections that persist beyond
628 the acute immune response exhibit prolonged circulation and increased splenic clearance (18)
629 allowed us to complement the model by Cao et al. (35) with an increased asexual parasite death
630 rate following the immuno-responsive period, which promoted the progressively increased
631 representation of sexual stages in later phases of the infection. Low gametocyte proportions early
632 on in infection can be explained by the fact that asexual replication efficiently increases while
633 adaptive immunity is absent and the lag of ~8 days of gametocyte development in the bone
634 marrow has its impact. In our model we propose that later immunity prevents fast asexual growth
635 and parasites persisting further are more efficiently removed in the spleen sustaining low
636 parasitaemias. By introducing these concepts into our model, we can observe the opposite lag
637 effect later in infection when the proportion of gametocytes finally reflects, despite keeping the
638 same sexual commitment rate, that of parasitaemias ~8 days earlier. In contrast, assuming
639 increased fractions of sexually committed parasites during the chronic phase of infection, our
640 model would predict a constant loss of parasitemia and eventual clearance of infection.
641 In conclusion, our data is consistent with a model in which *P. falciparum* maintains a constant rate
642 of sexual commitment such that the proportion of gametocytes increases over time as infection

643 persists and asexual parasite numbers decline more rapidly, a strategy that may help overcome
644 the vector-free period and increase transmission efficiency.
645

646 **Acknowledgments**

647 We thank the residents of Kalifabougou, Mali and Nangonera, Uganda for participating in the
648 studies. We acknowledge the support of the Flow Cytometry Core Facility of DKFZ, the Heidelberg
649 University Metabolomics Core Technology Platform, and the Clinical Lipidomics Unit of Mainz
650 University Medical Center. We thank Matthias Marti and Lauriane Sollelis at University of Glasgow
651 for help and expertise with in vitro induction of parasite sexual commitment and
652 gametocytogenesis. This work was supported by the European Research Council (ERC) under the
653 European Union's Horizon 2020 research and innovation programme (grant agreement No
654 759534), and the German Center for Infection research (DZIF). The Malian cohort study was
655 supported by the Division of Intramural Research, National Institute of Allergy and Infectious
656 Diseases of the National Institutes of Health; and the Ugandan study was supported by the
657 National Institutes of Health as part of the International Centers of Excellence in Malaria Research
658 program. Chica and Heinz-Schaller Foundation supported Frederik Graw.
659

660 **Competing Interest Statement**

661 The authors declare that they have no conflict of interest.
662

663 **References**

664 1. Grassi B, Bignami A, Bastianelli G. Medical Zoology: Further Researches upon the Cycle of
665 Human Malaria in the Body of the Mosquito. Ind Med Gaz. 1899;34(3):104-7.
666 2. Prudencio M, Rodriguez A, Mota MM. The silent path to thousands of merozoites: the
667 Plasmodium liver stage. Nat Rev Microbiol. 2006;4(11):849-56.
668 3. Haldar K, Murphy SC, Milner DA, Taylor TE. Malaria: mechanisms of erythrocytic infection and
669 pathological correlates of severe disease. Annu Rev Pathol. 2007;2:217-49.
670 4. Kafsack BF, Rovira-Graells N, Clark TG, Bancells C, Crowley VM, Campino SG, et al. A
671 transcriptional switch underlies commitment to sexual development in malaria parasites. Nature.
672 2014;507(7491):248-52.
673 5. Arnot DE, Gull K. The Plasmodium cell-cycle: facts and questions. Ann Trop Med Parasitol.
674 1998;92(4):361-5.
675 6. Bruce MC, Alano P, Duthie S, Carter R. Commitment of the malaria parasite Plasmodium
676 falciparum to sexual and asexual development. Parasitology. 1990;100 Pt 2:191-200.

677 7. Inselburg J. Gametocyte formation by the progeny of single Plasmodium falciparum schizonts. J
678 Parasitol. 1983;69(3):584-91.
679 8. Hawking F, Wilson ME, Gammage K. Evidence for cyclic development and short-lived maturity
680 in the gametocytes of Plasmodium falciparum. Trans R Soc Trop Med Hyg. 1971;65(5):549-59.
681 9. Li J, Shami GJ, Cho E, Liu B, Hanssen E, Dixon MWA, et al. Repurposing the mitotic machinery
682 to drive cellular elongation and chromatin reorganisation in Plasmodium falciparum gametocytes.
683 Nature Communications. 2022;13(1).
684 10. Parkyn Schneider M, Liu B, Glock P, Suttie A, McHugh E, Andrew D, et al. Disrupting assembly
685 of the inner membrane complex blocks Plasmodium falciparum sexual stage development. PLoS
686 Pathog. 2017;13(10):e1006659.
687 11. Farfour E, Charlotte F, Settegrana C, Miyara M, Buffet P. The extravascular compartment of the
688 bone marrow: a niche for Plasmodium falciparum gametocyte maturation? Malar J. 2012;11:285.
689 12. Tiburcio M, Silvestrini F, Bertuccini L, Sander AF, Turner L, Lavstsen T, et al. Early
690 gametocytes of the malaria parasite Plasmodium falciparum specifically remodel the adhesive
691 properties of infected erythrocyte surface. Cell Microbiol. 2013;15(4):647-59.
692 13. Smalley ME, Sinden RE. Plasmodium falciparum gametocytes: their longevity and infectivity.
693 Parasitology. 1977;74(1):1-8.
694 14. Gebru T, Lalremruata A, Kremsner PG, Mordmuller B, Held J. Life-span of in vitro differentiated
695 Plasmodium falciparum gametocytes. Malar J. 2017;16(1):330.
696 15. Billker O, Lindo V, Panico M, Etienne AE, Paxton T, Dell A, et al. Identification of xanthurenic
697 acid as the putative inducer of malaria development in the mosquito. Nature. 1998;392(6673):289-92.
698 16. Ross R. The role of the mosquito in the evolution of the malarial parasite: the recent researches
699 of Surgeon-Major Ronald Ross, I.M.S. 1898. Yale J Biol Med. 2002;75(2):103-5.
700 17. Dicko A, Klion AD, Thera MA, Sagara I, Yalcouye D, Niambele MB, et al. The etiology of severe
701 anemia in a village and a periurban area in Mali. Blood. 2004;104(4):1198-200.
702 18. Andrade CM, Fleckenstein H, Thomson-Luque R, Doumbo S, Lima NF, Anderson C, et al.
703 Increased circulation time of Plasmodium falciparum underlies persistent asymptomatic infection in the
704 dry season. Nat Med. 2020.
705 19. Babiker HA, Abdel-Muhsin AM, Ranford-Cartwright LC, Satti G, Walliker D. Characteristics of
706 Plasmodium falciparum parasites that survive the lengthy dry season in eastern Sudan where malaria
707 transmission is markedly seasonal. Am J Trop Med Hyg. 1998;59(4):582-90.
708 20. Portugal S, Tran TM, Ongoiba A, Bathily A, Li S, Doumbo S, et al. Treatment of Chronic
709 Asymptomatic Plasmodium falciparum Infection Does Not Increase the Risk of Clinical Malaria Upon
710 Reinfection. Clin Infect Dis. 2017;64(5):645-53.
711 21. Adomako-Ankomah Y, Chenoweth MS, Tocker AM, Doumbia S, Konate D, Doumbouya M, et
712 al. Host age and Plasmodium falciparum multiclonality are associated with gametocyte prevalence: a 1-
713 year prospective cohort study. Malar J. 2017;16(1):473.
714 22. Drakeley CJ, Secka I, Correa S, Greenwood BM, Targett GA. Host haematological factors
715 influencing the transmission of Plasmodium falciparum gametocytes to Anopheles gambiae s.s.
716 mosquitoes. Trop Med Int Health. 1999;4(2):131-8.
717 23. Gouagna LC, Bancone G, Yao F, Yameogo B, Dabire KR, Costantini C, et al. Genetic variation
718 in human HBB is associated with Plasmodium falciparum transmission. Nat Genet. 2010;42(4):328-31.
719 24. Price R, Nosten F, Simpson JA, Luxemburger C, Phaipun L, ter Kuile F, et al. Risk factors for
720 gametocyte carriage in uncomplicated falciparum malaria. Am J Trop Med Hyg. 1999;60(6):1019-23.
721 25. Barry A, Bradley J, Stone W, Guelbeogo MW, Lanke K, Ouedraogo A, et al. Higher gametocyte
722 production and mosquito infectivity in chronic compared to incident Plasmodium falciparum infections.
723 Nat Commun. 2021;12(1):2443.
724 26. Group WGS. Gametocyte carriage in uncomplicated Plasmodium falciparum malaria following
725 treatment with artemisinin combination therapy: a systematic review and meta-analysis of individual
726 patient data. BMC Med. 2016;14:79.
727 27. Rek J, Blanken SL, Okoth J, Ayo D, Onyige I, Musasizi E, et al. Asymptomatic school-aged
728 children are important drivers of malaria transmission in a high endemicity setting in Uganda. J Infect
729 Dis. 2022.
730 28. Tadesse FG, Slater HC, Chali W, Teelen K, Lanke K, Belachew M, et al. The Relative
731 Contribution of Symptomatic and Asymptomatic Plasmodium vivax and Plasmodium falciparum
732 Infections to the Infectious Reservoir in a Low-Endemic Setting in Ethiopia. Clin Infect Dis.
733 2018;66(12):1883-91.

29. Williams JL. Stimulation of Plasmodium falciparum gametocytogenesis by conditioned medium from parasite cultures. Am J Trop Med Hyg. 1999;60(1):7-13.
30. Dyer M, Day KP. Regulation of the rate of asexual growth and commitment to sexual development by diffusible factors from in vitro cultures of Plasmodium falciparum. Am J Trop Med Hyg. 2003;68(4):403-9.
31. Brancucci NMB, Gerdt JP, Wang C, De Niz M, Philip N, Adapa SR, et al. Lysophosphatidylcholine Regulates Sexual Stage Differentiation in the Human Malaria Parasite Plasmodium falciparum. Cell. 2017;171(7):1532-44 e15.
32. Filarsky M, Fraschka SA, Niederwieser I, Brancucci NMB, Carrington E, Carrio E, et al. GDV1 induces sexual commitment of malaria parasites by antagonizing HP1-dependent gene silencing. Science. 2018;359(6381):1259-63.
33. Campelo Morillo RA, Tong X, Xie W, Abel S, Orchard LM, Daher W, et al. The transcriptional regulator HDP1 controls expansion of the inner membrane complex during early sexual differentiation of malaria parasites. Nat Microbiol. 2022;7(2):289-99.
34. Thomson-Luque R, Votborg-Novel L, Ndovie W, Andrade CM, Niangaly M, Attipa C, et al. Plasmodium falciparum transcription in different clinical presentations of malaria associates with circulation time of infected erythrocytes. Nat Commun. 2021;12(1):4711.
35. Cao P, Collins KA, Zaloumis S, Wattanakul T, Tarning J, Simpson JA, et al. Modeling the dynamics of Plasmodium falciparum gametocytes in humans during malaria infection. Elife. 2019;8.
36. Painter HJ, Carrasquilla M, Llinas M. Capturing in vivo RNA transcriptional dynamics from the malaria parasite Plasmodium falciparum. Genome Res. 2017;27(6):1074-86.
37. Poran A, Notzel C, Aly O, Mencia-Trinchant N, Harris CT, Guzman ML, et al. Single-cell RNA sequencing reveals a signature of sexual commitment in malaria parasites. Nature. 2017;551(7678):95-9.
38. Lopez-Barragan MJ, Lemieux J, Quinones M, Williamson KC, Molina-Cruz A, Cui K, et al. Directional gene expression and antisense transcripts in sexual and asexual stages of Plasmodium falciparum. BMC Genomics. 2011;12:587.
39. Tran TM, Li S, Doumbo S, Doumtabe D, Huang CY, Dia S, et al. An intensive longitudinal cohort study of Malian children and adults reveals no evidence of acquired immunity to Plasmodium falciparum infection. Clin Infect Dis. 2013;57(1):40-7.
40. Meerstein-Kessel L, Andolina C, Carrio E, Mahamar A, Sawa P, Diawara H, et al. A multiplex assay for the sensitive detection and quantification of male and female Plasmodium falciparum gametocytes. Malar J. 2018;17(1):441.
41. Lasonder E, Rijpma SR, van Schaijk BC, Hoeijmakers WA, Kensche PR, Gresnigt MS, et al. Integrated transcriptomic and proteomic analyses of P. falciparum gametocytes: molecular insight into sex-specific processes and translational repression. Nucleic Acids Res. 2016;44(13):6087-101.
42. Surma MA, Herzog R, Vasilj A, Klose C, Christinat N, Morin-Rivron D, et al. An automated shotgun lipidomics platform for high throughput, comprehensive, and quantitative analysis of blood plasma intact lipids. Eur J Lipid Sci Technol. 2015;117(10):1540-9.
43. Lerner R, Post J, Loch S, Lutz B, Bindila L. Targeting brain and peripheral plasticity of the lipidome in acute kainic acid-induced epileptic seizures in mice via quantitative mass spectrometry. Biochim Biophys Acta Mol Cell Biol Lipids. 2017;1862(2):255-67.
44. Andolina C, Rek JC, Briggs J, Okoth J, Musiime A, Ramjith J, et al. Sources of persistent malaria transmission in a setting with effective malaria control in eastern Uganda: a longitudinal, observational cohort study. Lancet Infect Dis. 2021.
45. Briggs J, Teyssier N, Nankabirwa JI, Rek J, Jagannathan P, Arinaitwe E, et al. Sex-based differences in clearance of chronic Plasmodium falciparum infection. Elife. 2020;9.
46. Hofmann N, Mwingira F, Shekalaghe S, Robinson LJ, Mueller I, Felger I. Ultra-sensitive detection of Plasmodium falciparum by amplification of multi-copy subtelomeric targets. PLoS Med. 2015;12(3):e1001788.
47. Tran TM, Guha R, Portugal S, Skinner J, Ongoiba A, Bhardwaj J, et al. A Molecular Signature in Blood Reveals a Role for p53 in Regulating Malaria-Induced Inflammation. Immunity. 2019;51(4):750-65 e10.
48. Miller LH, Good MF, Milon G. Malaria pathogenesis. Science. 1994;264(5167):1878-83.
49. Klinger E, Rickert D, Hasenauer J. pyABC: distributed, likelihood-free inference. Bioinformatics. 2018;34(20):3591-3.

50. Ruhamyankaka E, Brunk BP, Dorsey G, Harb OS, Helb DA, Judkins J, et al. ClinEpiDB: an open-access clinical epidemiology database resource encouraging online exploration of complex studies. Gates Open Res. 2019;3:1661.
51. Eichner M, Diebner HH, Molineaux L, Collins WE, Jeffery GM, Dietz K. Genesis, sequestration and survival of Plasmodium falciparum gametocytes: parameter estimates from fitting a model to malariatherapy data. Trans R Soc Trop Med Hyg. 2001;95(5):497-501.
52. Tiburcio M, Dixon MW, Looker O, Younis SY, Tilley L, Alano P. Specific expression and export of the Plasmodium falciparum Gametocyte EXported Protein-5 marks the gametocyte ring stage. Malar J. 2015;14:334.
53. Usui M, Prajapati SK, Ayanful-Torgby R, Acquah FK, Cudjoe E, Kakaney C, et al. Plasmodium falciparum sexual differentiation in malaria patients is associated with host factors and GDV1-dependent genes (vol 10, 2140, 2019). Nature Communications. 2019;10.
54. Shanks GD. Hypothesis: dynamics of classical malaria epidemics show Plasmodium falciparum's survival strategy. Am J Trop Med Hyg. 2015;92(3):561-4.
55. Rono MK, Nyonda MA, Simam JJ, Ngoi JM, Mok S, Kortok MM, et al. Adaptation of Plasmodium falciparum to its transmission environment. Nat Ecol Evol. 2018;2(2):377-87.
56. Oduma CO, Ogolla S, Atieli H, Ondigo BN, Lee MC, Githeko AK, et al. Increased investment in gametocytes in asymptomatic Plasmodium falciparum infections in the wet season. BMC Infect Dis. 2021;21(1):44.
57. Rosenberg R, Andre RG, Ketrangsee S. Seasonal fluctuation of Plasmodium falciparum gametocytaemia. Trans R Soc Trop Med Hyg. 1990;84(1):29-33.
58. Gadalla AAH, Schneider P, Churcher TS, Nassir E, Abdel-Muhsin AMA, Ranford-Cartwright LC, et al. Associations between Season and Gametocyte Dynamics in Chronic Plasmodium falciparum Infections. Plos One. 2016;11(11).
59. Ouedraogo AL, de Vlas SJ, Nebie I, Ilboudo-Sanogo E, Bousema JT, Ouattara AS, et al. Seasonal patterns of Plasmodium falciparum gametocyte prevalence and density in a rural population of Burkina Faso. Acta Trop. 2008;105(1):28-34.
60. Ouedraogo AL, Goncalves BP, Gneme A, Wenger EA, Guelbeogo MW, Ouedraogo A, et al. Dynamics of the Human Infectious Reservoir for Malaria Determined by Mosquito Feeding Assays and Ultrasensitive Malaria Diagnosis in Burkina Faso. J Infect Dis. 2016;213(1):90-9.
61. Portugaliza HP, Miyazaki S, Geurten FJ, Pell C, Rosanas-Urgell A, Janse CJ, et al. Artemisinin exposure at the ring or trophozoite stage impacts Plasmodium falciparum sexual conversion differently. Elife. 2020;9.
62. Orikiiriza J, Surowiec I, Lindquist E, Bonde M, Magambo J, Muhinda C, et al. Lipid response patterns in acute phase paediatric Plasmodium falciparum malaria. Metabolomics. 2017;13(4):41.
63. Portugaliza HP, Natama HM, Guetens P, Rovira-Vallbona E, Some AM, Millogo A, et al. Plasmodium falciparum sexual conversion rates can be affected by artemisinin-based treatment in naturally infected malaria patients. EBioMedicine. 2022;83:104198.
64. Greischar MA, Mideo N, Read AF, Bjornstad ON. Quantifying Transmission Investment in Malaria Parasites. PLoS Comput Biol. 2016;12(2):e1004718.
65. Prajapati SK, Ayanful-Torgby R, Pava Z, Barbeau MC, Acquah FK, Cudjoe E, et al. The transcriptome of circulating sexually committed Plasmodium falciparum ring stage parasites forecasts malaria transmission potential. Nat Commun. 2020;11(1):6159.
66. Collins WE, Jeffery GM. A retrospective examination of sporozoite- and trophozoite-induced infections with Plasmodium falciparum: development of parasitologic and clinical immunity during primary infection. Am J Trop Med Hyg. 1999;61(1 Suppl):4-19.

Figure 1

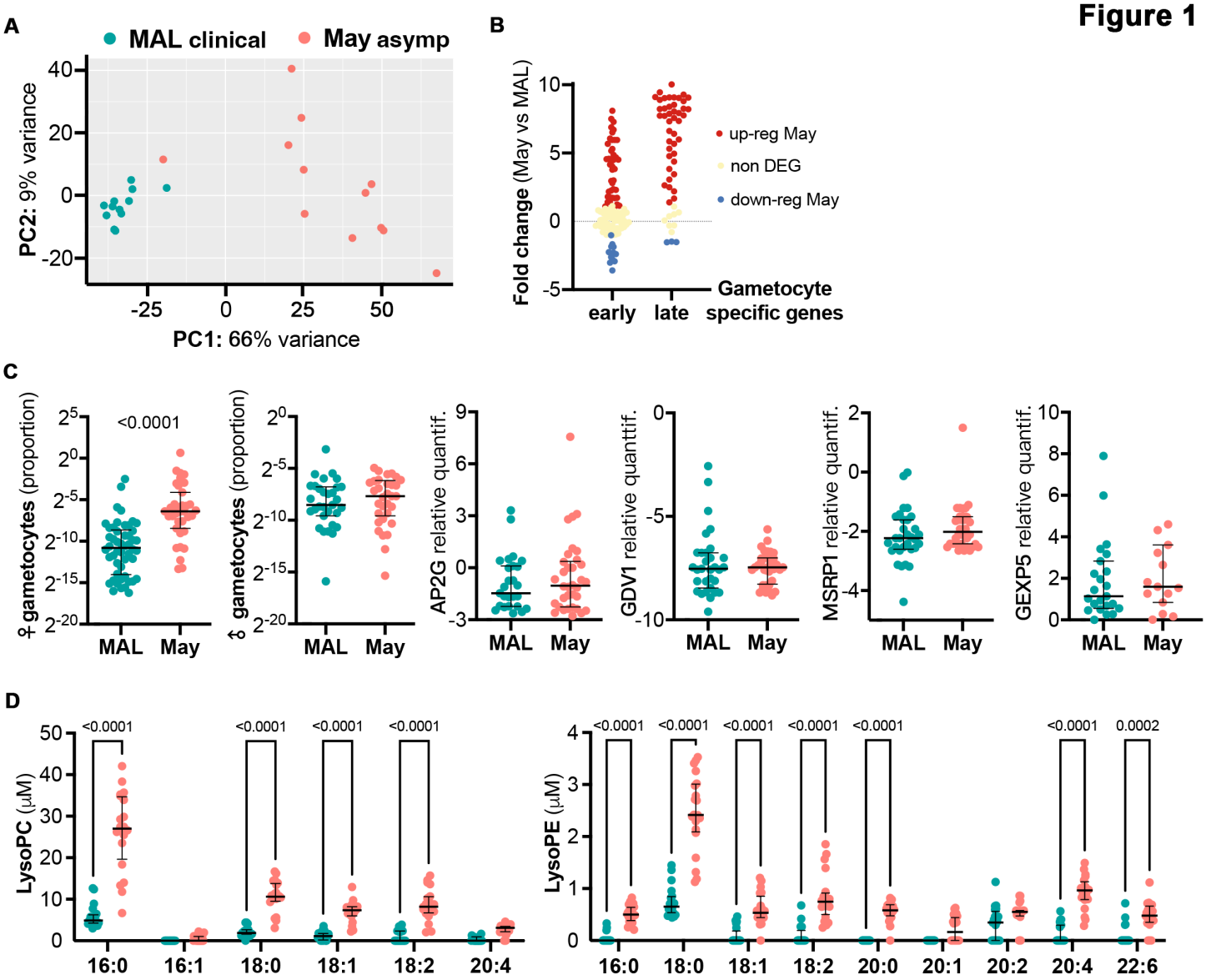
A
MAL clinical
May asymp
PC2: 9% variance
PC1: 66% variance
B
Fold change (May vs MAL)
up-reg May
non DEG
down-reg May
early
late
Gametocyte specific genes
C
♀ gametocytes (proportion)
<0.0001
♂ gametocytes (proportion)
AP2G relative quantif.
GDV1 relative quanttif.
MSRP1 relative quantif.
GEXP5 relative quantif.
MAL
May
D
LysoPC (μM)
LysoPE (μM)
16:0
16:1
18:0
18:1
18:2
20:4
20:0
20:1
20:2
22:6
0.0002

Figure 2

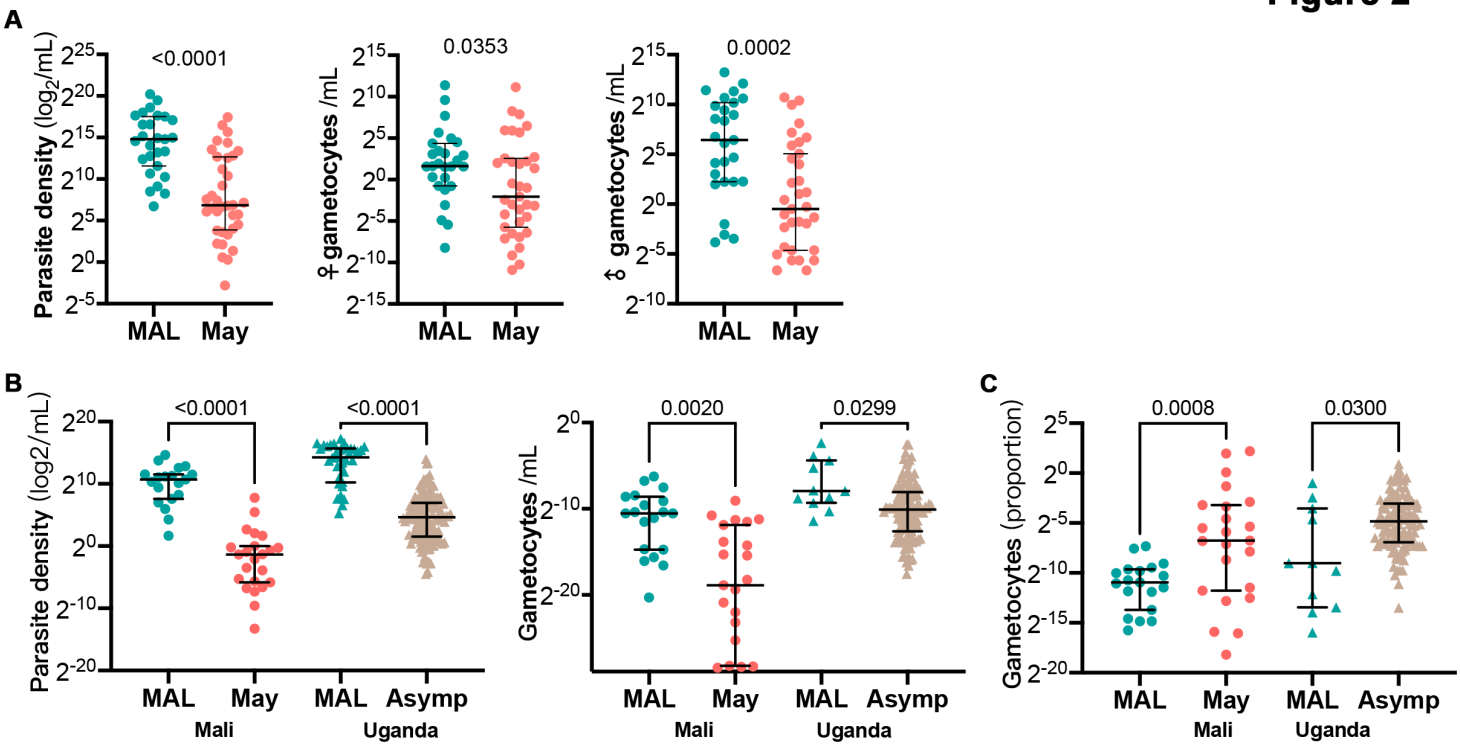
A
Parasite density (log2/mL)
<0.0001
MAL
May
♀gametocytes /mL
0.0353
♂ gametocytes /mL
0.0002
B
Parasite density (log2/mL)
<0.0001
<0.0001
MAL
May
MAL
Asymp
Mali
Uganda
Gametocytes /mL
0.0020
0.0299
C
Gametocytes (proportion)
0.0008
0.0300

Figure 3

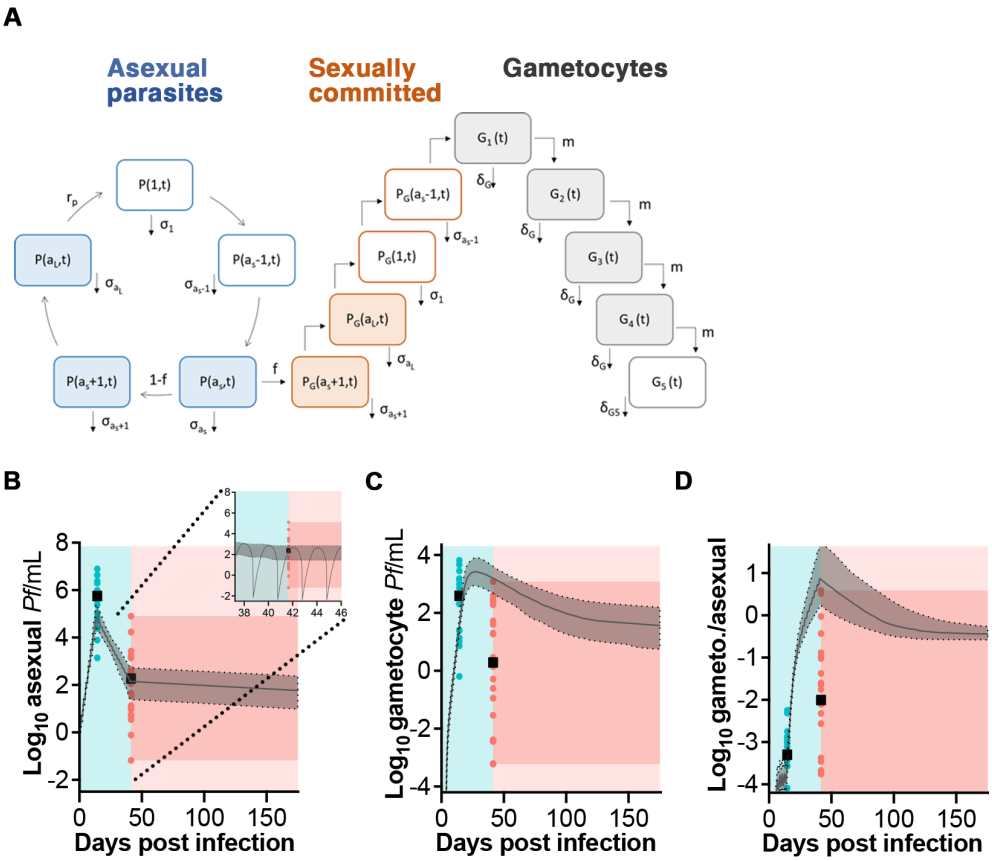
A
Asexual parasites
Sexually committed
Gametocytes
P(1,t)
P(a_L,t)
P(a_s-1,t)
P(a_s+1,t)
P(a_L,t)
1-f
f
P_G(a_s-1,t)
P_G(1,t)
P_G(a_L,t)
P_G(a_s+1,t)
G_1(t)
G_2(t)
G_3(t)
G_4(t)
G_5(t)
m
B
C
D
Log10 asexual Pf/mL
Log10 gametocyte Pf/mL
Log10 gameto./asexual
Days post infection

Supplementary Figure 1

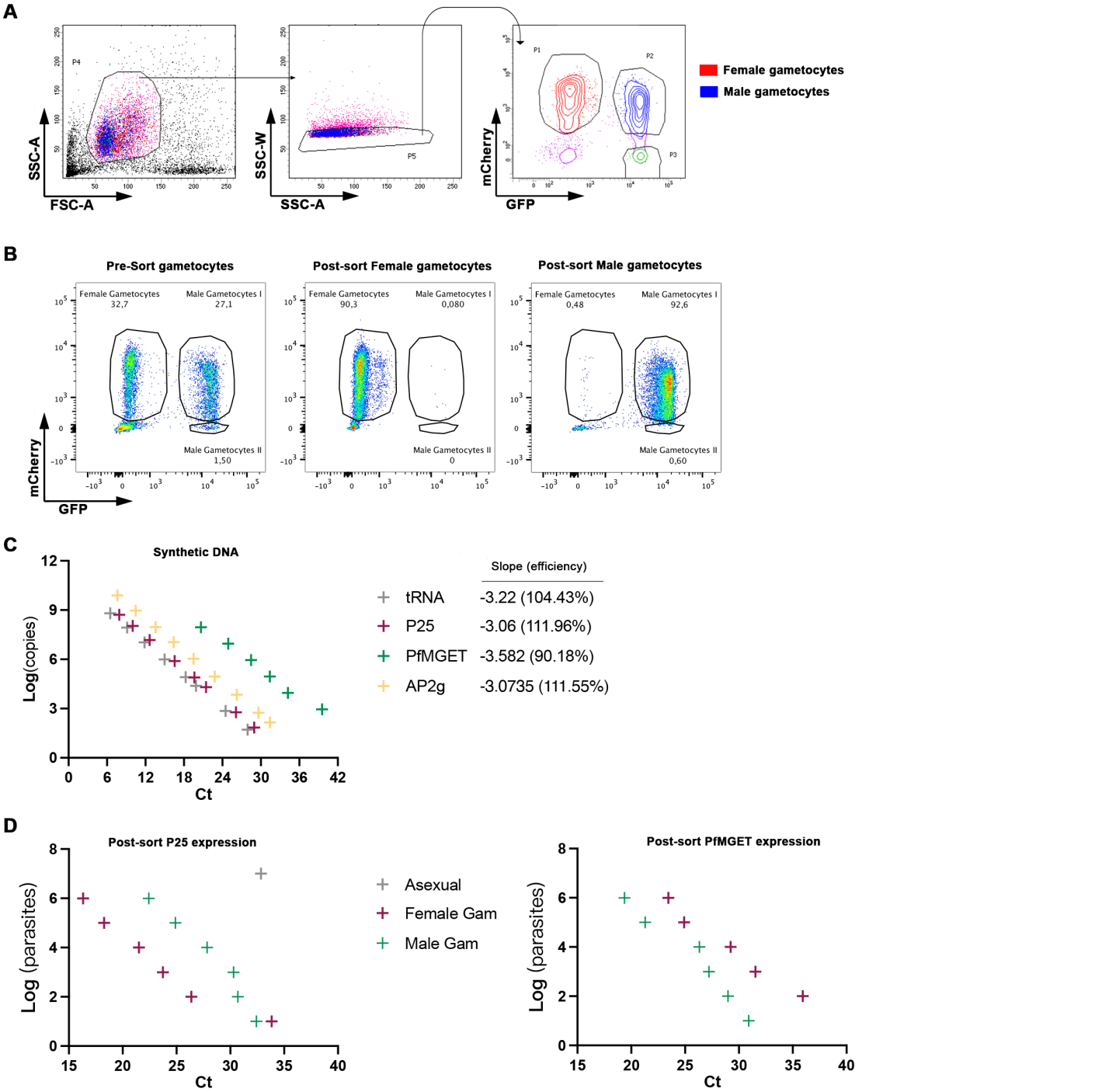

Supplementary Figure 2

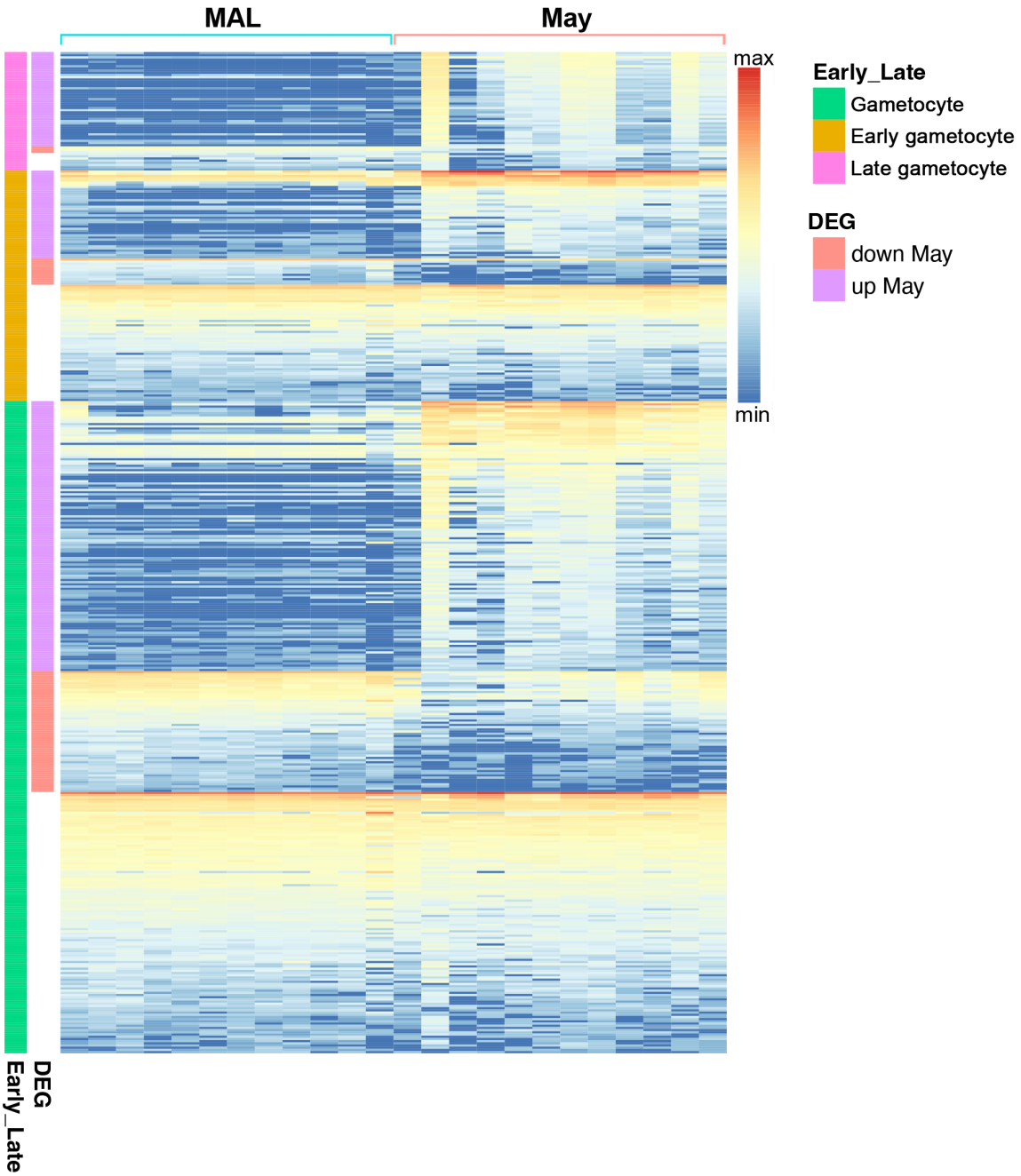

Supplementary Figure 3

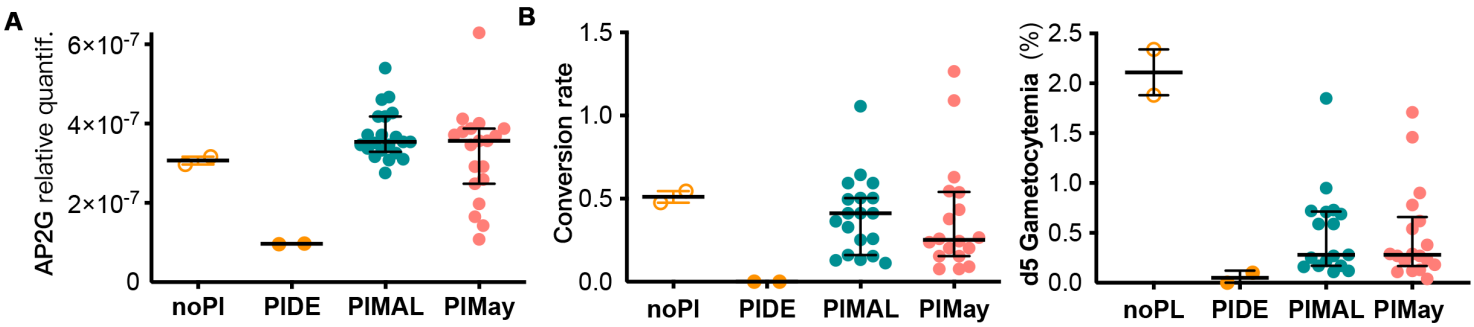

Supplementary Figure 4

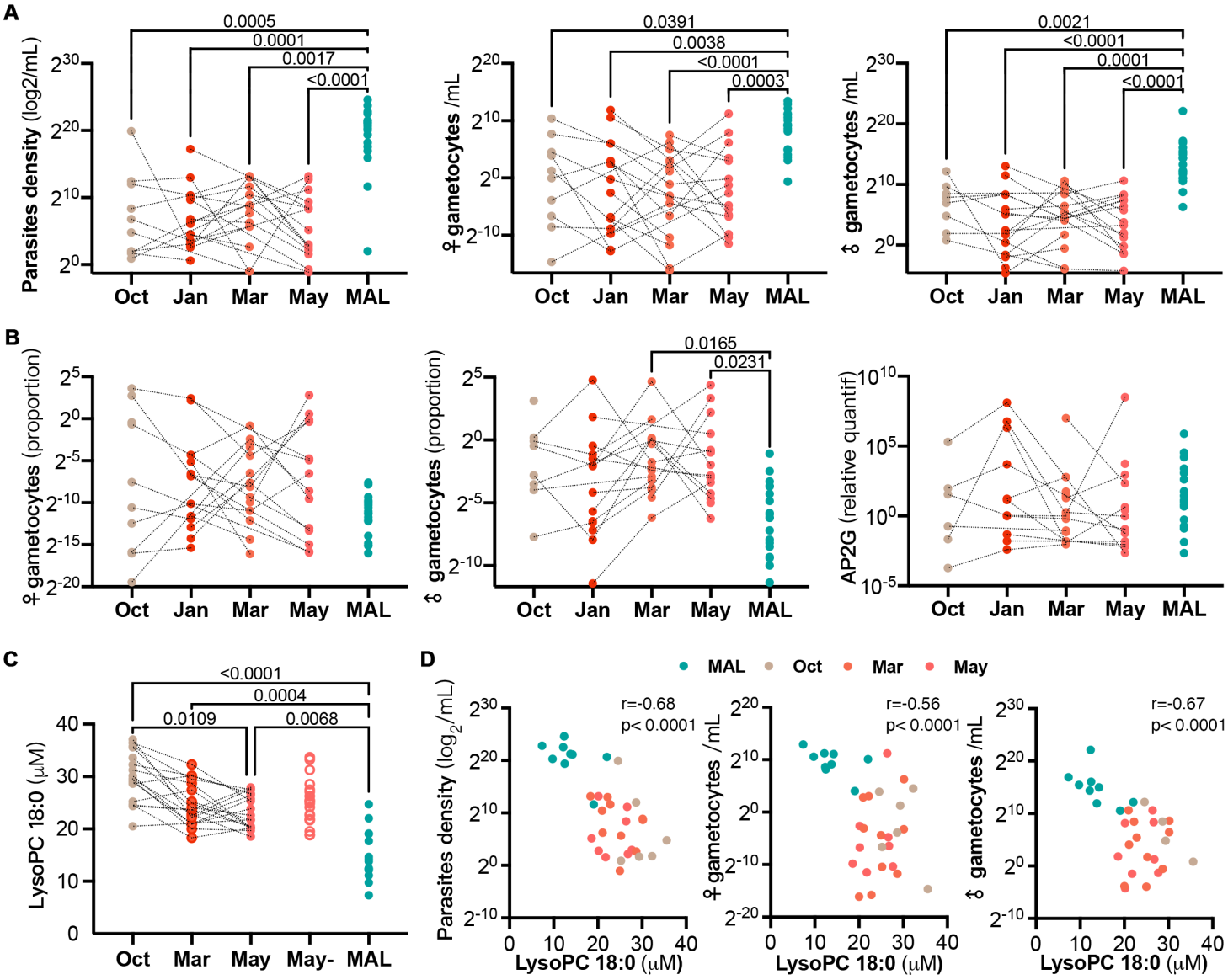

Supplementay Figure 5

A

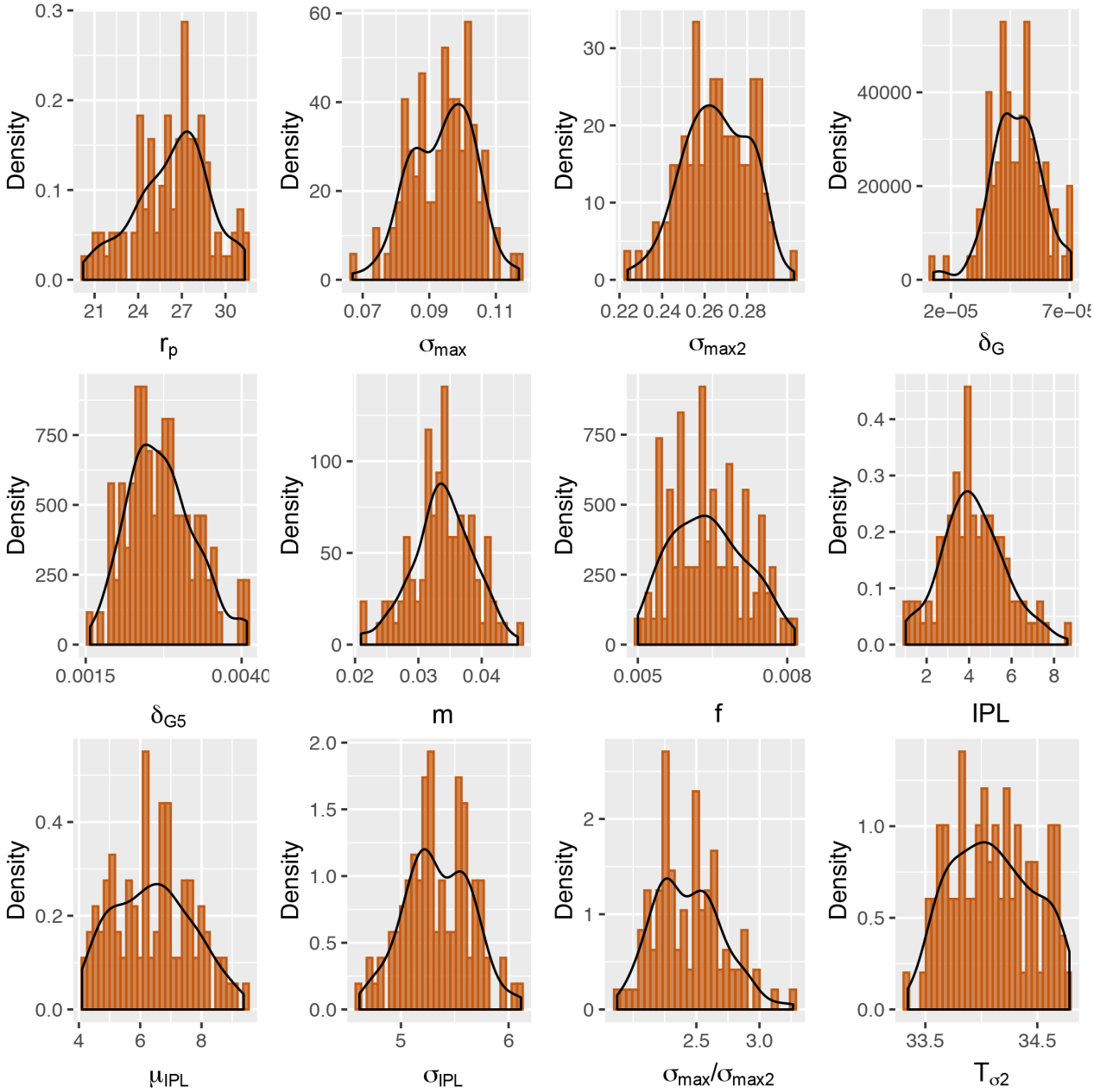

B

	Acute Phase	Transition phase	Chronic phase
Sexual commitment rate	0.54 - 0.76 %		
Gametocyte circulation time	12.04 - 22.28 days		
Parasite multiplication factor / 48 h	3.87 - 8.18	0.33 - 1.38	0.50 - 2.29
Gametocyte sequestration time	3.89 - 6.04 days		

Spplemantary Figure 6

A

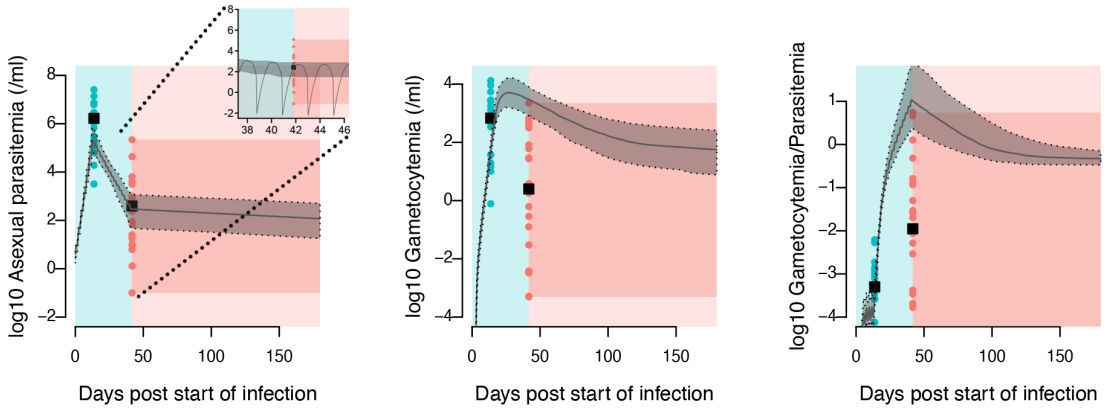

B

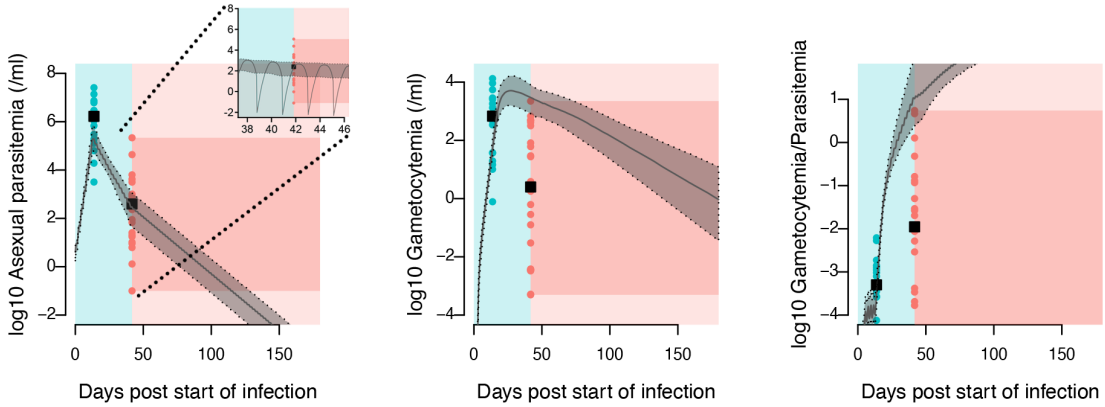

Figure legends

Figure 1. *P. falciparum* transcription and quantification of gametocyte density and proportions. A, Principal components analysis of RNA-Seq data of 333 gametocyte specific *P. falciparum* genes from parasites collected at the end of the dry season and from clinical malaria cases (n= 12 May, 12 MAL). **B**, Fold change between parasites collected at the end of the dry season and from clinical malaria cases (n= 12 May, 12MAL) of early and late gametocyte transcripts according to López-Barragán et al., 2011; Poran et al., 2017 and Petter unpublished data. Each dot represents a gene and color identifies range in fold change, red: upregulated in May, yellow: not DEG, and blue: downregulated in May). **C,** Proportion of female (♀) and male (♂) gametocytes, relative expression of AP2G, GDV1, MSRP1, and GEXP5, detected by qRT-PCR of RDT+ subclinical children at the end of the dry season (May n > 15) and of children with their first clinical malaria episode (MAL n > 23) in the wet season. **D,** Plasma concentration of Lyso-PC (left) and Lyso-PE (right) species of RDT^+ subclinical children at the end of the dry season (May) and of children with their first clinical malaria episode (MAL) in the wet season. Lipid data represented as median ± IQR; two-way ANOVA with Tukey multiple comparisons correction. Parasitaemia and gametocytemia and AP2G, GDV1, MSRP1, and GEXP5 expression data represented as median ± IQR; Mann-Whitney test.

Figure 2. *P. falciparum* gametocyte density is higher clinical cases of malaria than in asymptomatic infection regardless of seasonality. A: Asexual parasite (left), Female (center) and male (right) density detected by qRT-PCR of RDT^+ subclinical children at the end of the dry season (May = 35) and of children with their first clinical malaria episode (MAL = 27) in the wet season. D: gametocyte **B**, Parasite (left) and gametocyte (right) densities detected by qRT-PCR of symptomatic (MAL n = 19 and 38 in Mali and Uganda respectively) and asymptomatic infections (May n = 23 and Asymp n = 122) in Mali and Uganda. **C**, Gametocyte proportion detected by qRT-PCR of symptomatic (MAL n = 19 and 38 in Mali and Uganda respectively) and asymptomatic

infections (May n = 23 and Asymp n = 122) in Mali and Uganda. Data represented as median ± IQR; multiple non-parametric test with Tukey-correction for multiple comparisons.

Fig 3 | Progressing infection leads to apparent differences in gametocytogenesis. A, Diagram of the mathematical model to describe parasite dynamics including individual compartments, transitions and death rates; Asexual parasites (P) replicate in a 48 h cycle, being cleared at an age dependent death rate (σ_a). A fraction of asexual parasites (f) transitions to the sexually committed parasite compartment (P_G), goes through a round of replication and develops into gametocytes (G). Gametocytes mature over 5 distinct stages in independent model compartments. Asexual parasites (blue), sexually committed parasites (orange) and gametocytes (grey) are indicated shaded if not circulating due to sequestration. **B**, Model prediction and clinical data of asexual parasites. The small inlay indicates a zoom-in showing the oscillating parasite dynamics within 48 h-intervals. **C**, Gametocytes density and **D**, proportion of gametocytes per mL blood. Individual data points and median (black square) of wet (aqua circles) and dry (orange circles) season data throughout acute (aqua shaded area) and chronic (salmon shaded area) phase of infection are shown. Median fit (grey line) and 95% prediction interval of 100 model predictions of the 6th PyABC generation are shown as grey shaded area.

Figure supplement legends

Supplementary Figure 1

A, Flow cytometry gating strategy to identify and sort PfDynGFP/ PfP47 gametocytes by mCherry and GFP expression into three populations (female: mCherry-positive, male I: mCherry- GFP-positive, male II: GFP-positive). **B,** Pre-sort gametocyte distribution, and post-sorting purity verification of female and male gametocytes. **C,** Serial dilutions of P25, PfMGET, AP2g, and Glycine-tRNA ligase synthetic DNA to determine curves' slopes and primer efficiency by qPCR. **D,** Standard curves determined with serial dilutions of sorted-purified female and male gametocytes, showing expression of female marker P25 (left) and male marker PfMGET (right).

54

55 **Supplementary Figure 2**

56 Heatmap showing normalized reads of 456 gametocyte specific genes of *P. falciparum* (rows) for
57 each subject (columns) collected at the end of the dry season (May) and at the first clinical malaria
58 case (MAL) in the ensuing transmission season.

59

60 **Supplementary Figure 3**

61 **A,** Relative expression of AP2G detected by qRT-PCR of Pf2004 24 h after 24 h culture with 25%
62 plasma collected during clinical malaria episodes (MAL n = 21), or at the end of the dry season
63 (May n = 19). **B,** Pf2004 conversion rate (gametocytes d5/parasites d2) (left) and gametocyte
64 density (right) detected by microscopy, after 24 h culture with 25% plasma collected during clinical
65 malaria episodes in the wet season (MAL n = 19) or at the end of the dry season (May n = 18),
66 alongside no plasma (noPl) and German (PIDE) conditions. Data represented as median ± IQR;
67 Mann-Whitney test.

68

69 **Supplementary Figure 4**

70 **A**, Density of total parasites (left), Female (centre), and male (right) gametocytes detected by qRT-
71 PCR of RDT^+ subclinical children at different times during the wet (Oct n = 10) and the dry season
72 (Jan, Mar and May n > 15), and during clinical malaria episodes (MAL n = 19). **B.** Proportion of
73 female (left) and male (centre) gametocytes, and relative expression of AP2G (right) determined by
74 qRT-PCR of RDT^+ subclinical children at different times during the wet (Oct n = 6) and the dry
75 season (Jan, Mar and May n > 11), and during clinical malaria episodes (MAL n = 19). **D.** Plasma
76 concentration of Lyso-PC 18:0 of RDT^+ subclinical children at different times during the wet (Oct n =
77 17) and the dry season (Mar and May n = 19), and during clinical malaria episodes (MAL n = 15).
78 Parasite gene expression and lipid data were compared through Kruskal-Wallis test with multiple
79 comparisons. **D**, Correlation between Lyso-PC 18:0 and parasite (left), female gametocyte (centre)
80 or male gametocyte (right) densities detected by qRT-PCR detected by qRT-PCR of RDT^+

81 subclinical children at different times during the wet (Oct n = 10) and the dry season (Mar and May
82 n > 15), and during clinical malaria episodes (MAL n = 19). *P* and r determined by Pearson
83 correlation
84
85 **Supplementary Figure 5**
86 **A,** Posterior distribution of 12 model parameters generated of 100 fits of 6th pyABC generation of
87 one representative pyABC fitting run. **B,** Estimates of biological parameters in distinct phases of P.
88 falciparum infection shown as 89% credibility interval of the posterior distributions. Sexual
89 commitment rate was calculated by fx100%. The parasite multiplication factor is calculated by exp(-
90 a_L)(1-f) with the term exp(-a_L)(1-f) describing the fraction of surviving asexual parasite after death
91 and sexual conversion per replication cycle. Gametocyte sequestration time was calculated by 4/m
92 in relation to the 4 sequestered states (stage I to IV) (Cao et al. 2019). While calculations of the
93 model where done in 1 h increments, all estimates shown in S3 Figure. B are converted to per day.
94
95 **Supplementary Figure 6**
96 Model prediction and clinical data of asexual parasites and gametocytes with variable sexual
97 commitment rate during asymptomatic phase of infection. Asexual parasites, oscillating parasite
98 dynamics within 48h interval, gametocytes and the proportion of gametocytes per mL blood are
99 shown for sexual commitment (f) 2% in **A** and 20% in **B** during chronic phase of infection.
100 Individual data points and median (black square) of wet (aqua circles) and dry (orange circles)
101 season data throughout acute (aqua shaded area) and chronic (salmon shaded area) phase of
102 infection are shown. Median fit (grey line) and 95% prediction interval of 100 model predictions of
103 the 6th PyABC generation are shown as grey shaded area.
104
105 **Table supplement legends**
106 **S1 Table.** Gene Ids and descriptions of transcripts defined as gametocyte-specific by Painter et al.,
107 2017; transcripts detected in RNA sequencing dataset (Andrade et al., 2020) comparing persistent

108 *P. falciparum* in at the end of the dry season (May) to *P. falciparum* of clinical malaria in the wet
109 season (MAL); and transcripts defining early or late gametocyte development gathered from Poran
110 et al., 2017 after request from the corresponding author, López-Barragán et al., 2011, and Jeninga
111 et al., unpublished. (pink and blue shaded rows highlight transcripts up or down regulated in May
112 vs. MAL, respectively.)
113
114 **S2 Table.** Key Resources Table
115